COMPUTATIONAL ASPECTS OF SOME ENTRANCE REGION FLOW PROBLEMS

by

CHING-TAI LU

B.S., Taiwan Provincial Cheng-Kung University, 1958
Tainan, Taiwan

A MASTER'S REPORT

submitted in partial fulfillment of the

requirements for the degree

MASTER OF SCIENCE

Department of Mechanical Engineering

KANSAS STATE UNIVERSITY
Manhattan, Kansas

1967

Approved by:

Ching-Lai Hwang
Major Professor

TABLE OF CONTENTS

page

NOMENCLATURE iii

CHAPTER 1. INTRODUCTION 1

References 3

CHAPTER 2. SCHILLER'S METHOD 5

2.1. Description of the Method 5

2.2. Computational Procedures 12

2.3. Results 18

2.4. Sample Calculation with Dimensions 23

References 25

CHAPTER 3. LANGHAAR'S LINEARIZING APPROXIMATE METHOD . . . 26

3.1. Description of the Method 26

3.2. Computational Procedures 31

3.3. Results and Discussion 66

References 69

CHAPTER 4. SCHLICHTING'S MATCHING METHOD 70

4.1. Description of the Method 70

4.2. Computational Procedures 78

4.3. Results and Discussion 113

References 115

ACKNOWLEDGEMENT 116

NOMENCLATURE

a	Channel half-height
A	Cross-sectional area of the tube
D	Tube diameter
g_x	x-component of the acceleration of gravity
p	Fluid pressure
p_0	Pressure at channel mouth
p_∞	Pressure at far upstream where fluid velocity is zero
Δp	Total pressure drop in the entrance region
P	Dimensionless pressure, $\frac{(p-p_0)}{\rho \bar{u}^2}$
R	Dimensionless radial coordinate, $\frac{r}{r_0}$
Re_a	Reynolds number, $\frac{\rho \bar{u} a}{\mu}$
Re_D	Reynolds number, $\frac{\rho \bar{u} D}{\mu}$
Re_r	Reynolds number, $\frac{\rho \bar{u} r_0}{\mu}$
r_0	Tube radius
t	Time
u, v, w	x,y,z-components of the velocity field
$\bar{u}$	Average velocity
u_c	Center line velocity
U	Dimensionless velocity in x-direction, $\frac{u}{\bar{u}}$
u_f	Velocity at fully developed condition
u^*	Deviation velocity
x, y, z	Rectangular coordinates
X	Dimensionless x-coordinate, $\frac{\mu x}{\rho a^2 \bar{u}} = \frac{(x/a)}{Re_a}$
x_e	Entrance length

X_e	Dimensionless entrance length, $\frac{(x_e/a)}{Re_a}$
Y	Dimensionless y-coordinate, $\frac{y}{a}$
ν	Kinematic viscosity
ρ	Fluid density
μ	Dynamic viscosity
δ	Boundary layer thickness
τ_w	Shear stress at the wall
ε	Dimensionless x-coordinate, $(\frac{\nu x}{a^2 \bar{u}})^{\frac{1}{2}}$
ε_*	Dimensionless x-coordinate at matching section

CHAPTER 1. INTRODUCTION

When a viscous fluid enters a conduit (a circular tube or a flat duct) the velocity profile of the flow changes as the flow progresses from the entrance to the interior of the conduit because the wall of the conduit tends to retard the flow. Eventually, the velocity profile will assume a form which is invariant with respect to the direction of flow. The flow in this region of changing velocity profile is the so-called hydrodynamic entrance region flow.

A study of the velocity field and friction factor in the entrance region of tubes and ducts is of practical importance and has been a subject of investigation for the last hundred years. In the study of the entrance region flow we usually wish to obtain expressions for (a) the velocity distribution at any section, (b) the pressure drop between any two sections, and (c) the value of the entrance length at which the fully developed flow may be said to be attained.

Although the governing differential equations for the entrance region flow can be easily written, their exact analytical solutions have not as yet been found. The celebrated boundary layer theory was published in 1904 by Prandtl. The equation of motion for the entrance region flow can be simplified considerably if such flow is approximated by a model based on the boundary layer theory. Although the boundary layer equations are much simpler than the original equations of motion, we are still unable to obtain their exact analytical solutions. Thus various approximation methods of solution have been employed to solve the entrance region flow problem. A thorough review and classification of the literature of this subject has been made by Hwang and Fan [1]*.

The approximate solutions may be classified into four general categories — the momentum integral method of Schiller [4], the linearization method of Langhaar [5] and Targ [6], the matching method of Schlichting [7], and the finite difference method [8]. These approximate methods are explained in detail in Li's report [9]. However, the numerical calculations of the solutions are not carried out in Li's report.

The purpose of this report is the detailed study of the entrance region flow phenomena by obtaining the numerical results with a high speed computer. Three methods including Schiller's momentum integral method [4], Langhaar's linearizing method [5], and Schlichting's matching method [7] are studied numerically. A series of numerical analyses including the evaluation of modified Bessel functions [10], numerical integration [11, 13, 14] series solution of differential equations, eigenvalue solution [12] and others are employed in this report.

The details of the numerical analysis, computational procedures, flow charts, FORTRAN programs and numerical results are presented.

---

* Numerals in brackets refer to references at the end of each chapter.

REFERENCES

1. Hwang, C. L. and Fan, L. T., "Bibliography of Hydrodynamic Entrance Region Flow", Special Report No. 67, Engineering Experiment Station, Kansas State University, March 1966.

2. Schlichting, H., "Boundary Layer Theory", McGraw-Hill, New York, 4th ed., 1960.

3. Goldstein, S. (editor), "Modern Developments in Fluid Dynamics", Vol. 1, Clarendum Press, Oxford, England, 1938, also Dover Pub., New York, 1965.

4. Schiller, L., "Die Entwicklung der laminaren Geschwindigkeitsverteilung und ihre Bedeutung für Zahigkeitmessungen", ZAMM, 2, 96-106, 1922.

5. Langhaar, H. L., "Steady Flow in the Transition Length of a Straight Tube", Trans. of ASME, J. of Appl. Mech., 64, A-55-58, 1942.

6. Targ, S. M., "Osnovaye zadachi teorii laminaraykh techenii (Fundamental Problems in the Theory of Laminar Flow)", GITTL, 1951.

7. Schlichting, H., "Laminare Kanaleinlanfströmung", ZAMM, 14, 368-373, 1934.

8. Hwang, C. L. and L. T. Fan, "A Finite Difference Analysis of Laminar Magnetohydrodynamic Flow in the Entrance Region of a Flat Rectangular Duct", Appl. Sci. Res. Sec. B, 10, 329-343 (1963).

9. Li, K. C., "Analytical and Numerical Solutions of Some Entrance Region Flow Problems", M.S. Report, Mech. Engg., Kansas State Univ., Jan. 1966.

10. Abramowitz, Milton and Stegun, Irene A., "Handbook of Mathematical Functions with Formulas, Graphs, and Mathematical Tables", (AMS 55), June 1964.

11. Bennett, Milne, Bateman, "Numerical Integration of Differential Equations", Dover Publications, Inc., 1956.

12. McCormick, J. M. and Salvadori, M. G., "Numerical Methods in FORTRAN", Prentice-Hall, Inc., Englewood Cliffs, New Jersey, 1964.

13. Henrici, P., "Elements of Numerical Analysis", John Wiley & Sons, Inc., New York, London, Sydney, 1964.

14. Nielson, K. L., "Methods in Numerical Analysis", 2nd ed., Macmillan Company, New York, 1964.

CHAPTER 2. SCHILLER'S METHOD

2.1. Description of the Method

Schiller's method is also known as the Karman-Pohlhausen momentum-integral method. When a viscous fluid enters a circular tube with a uniform velocity profile across the cross-section, a thin boundary layer is often considered to have been formed. This is mentioned in the previous chapter. The thickness of this layer increases with the distance from the entry until it is equal to the radius of the pipe. Outside the boundary layer, the flow is considered to be frictionless and accelerated. In this method the velocity profile is assumed to be a curve built-up by two parabolas and a straight line (see Fig. 2.1); the vertices of the parabolas lie on the border of the boundary layer. The parabolic velocity in the boundary layer is assumed to be

$$\frac{u}{u_0} = 2\left(\frac{y}{\delta}\right) - \left(\frac{y}{\delta}\right)^2 \qquad (1)$$

where

$$y = r_0 - r$$

and u_0 is the velocity of the central core and is a function of x; δ is the thickness of the boundary layer.

The equation of continuity and the equation of motion (the momentum equation) give two relations among u_0, x, and δ. Elimination of δ will lead to a relation between u_0 and x.

The momentum theory is used here for the x direction to ob-

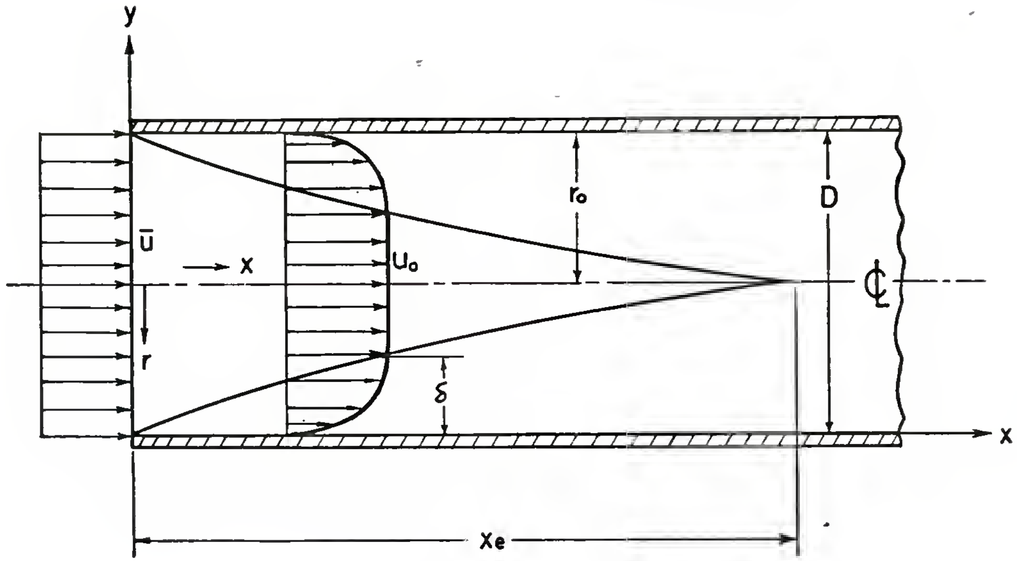

Fig. 2.1. Velocity profile in the entrance region of a circular tube.

tain a momentum integral equation representing the equation of motion. The control surface is formed by two planes a-b and c-d, spaced apart from each other by the small distance dx and by the wall (see Fig. 2.2). By means of the momentum balance on this control surface the following momentum integral equation is obtained.

$$\frac{d}{dx}\left[\int_0^{\delta} u^2(r_0 - y)dy\right] - u_0 \frac{d}{dx}\left[\int_0^{\delta} u(r_0 - y)dy\right]$$

$$= -2\nu u_0\left(\frac{r_0}{\delta}\right) + \frac{1}{2} r_0^{2} \left[2 \frac{\delta}{r_0} - \left(\frac{\delta}{r_0}\right)^2\right] u_0 \frac{du_0}{dx} . \qquad (2)$$

Substituting the assumed velocity profile expressed by equation (1) into the integral form of the continuity equation and carrying out the integration, we obtain a relation between the boundary layer thickness, δ, and the center line velocity, u_0, as shown below:

$$\frac{\delta}{r_0} = 2 - \sqrt{4 - 6\left(1 - \frac{\bar{u}}{u_0}\right)} \qquad (3)$$

where $\bar{u}$ is the average velocity.

Substituting equations (1) and (3) into equation (2), and carrying out the integration, we obtain a relation between u_0 and x as follows:

$$\frac{x/D}{Re_D} = \frac{1}{16}\left[\frac{58}{15}\eta - \frac{22}{5} \ln(1+\eta) - \frac{17}{15}\sqrt{4+2\eta-2\eta^2}\right.$$

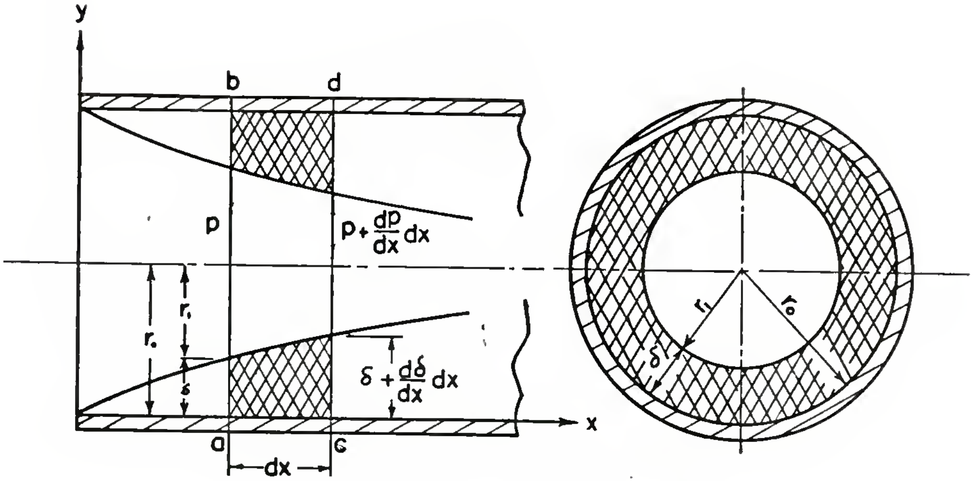

Fig. 2.2. Region for deriving the momentum integral equation.

$$- \frac{16}{5}\sqrt{\frac{4-2\eta}{1+\eta}} - \frac{37\sqrt{2}}{10}\sin^{-1}\left(\frac{2\eta-1}{3}\right)$$

$$- \frac{37\sqrt{2}}{10}\sin^{-1}\left(\frac{1}{3}\right) + \frac{26}{3}\Big] \qquad (4)$$

where

$$\eta = \frac{u_0}{\bar{u}} - 1 .$$

Therefore the velocity profile in the entrance region is defined by equations (1), (3), and (4). Given a value of u_0, the values of x and δ are known from equations (4) and (3). The velocity distribution at the corresponding section is defined by equation (1). The flow is fully developed when $\delta = r_0$ and $u_0 = 2\bar{u}$. Hence $\eta = 1$. Then from equation (4), the entrance length is found to be

$$x_e = 0.02877\ DRe_D .$$

Differentiating both sides of equation (4) with respect to x, we see that $\frac{d\eta}{dx}$, that is $\frac{du_0}{dx}$, does not vanish at $\eta = 1$. This means that the center line velocity does not asymptotically approach its final value, $2\bar{u}$, at the fully developed section.

For the calculation of the pressure drop in the entrance region, the Bernoulli equation is applied since it is assumed that a potential flow in the central core exists throughout the entrance region. Therefore, the pressure distribution is assumed to be dependent only on the potential flow. The pressure drop between any two locations in this region is expressed as

$$p_1 - p_2 = \frac{\rho}{2}\left[(u_0)_2{}^2 - (u_0)_1{}^2\right] = \frac{\rho}{2}\bar{u}^2\left[(\eta_2{}^2 - \eta_1{}^2) + 2(\eta_2 - \eta_1)\right] . \qquad (5)$$

Since $x = 0$ and $\eta_0 = 0$ at the entry, and $x = x_e$ and $\eta = 1$ at the fully developed section, the total pressure drop in the entrance region is

$$\Delta p = \frac{3}{2}\rho\bar{u}^2 .$$

The pressure drop in the entrance region is larger than that in the fully developed region of equal length because of the increased friction loss and the fact that the kinetic energy of the fluid increases as it passes downstream. For the evaluation of total pressure drop between a section in the entrance region and a section in the fully developed region, it is more convenient to treat the entrance region as a fully developed one and the pressure drop thus calculated is modified by a correction factor. The equation for calculating the total pressure drop in the fully developed section is found to be

$$\frac{p_0 - p}{\frac{\rho\bar{u}^2}{2}} = \frac{64}{Re_D}\frac{x}{D} + 1.16$$

where 1.16 is the correction factor. If the fluid enters the pipe from a region where the pressure is p_∞ and the velocity is negligible, there is a pressure drop of $\frac{1}{2}\rho\bar{u}^2$, and then the total pressure drop is

$$\frac{p_\infty - p}{\frac{\rho \bar{u}^2}{2}} = \frac{64x}{Re_D D} + 2.16 .$$

The derivation and solution are given in detail in Li's report [2].

2.2. Computational Procedures

To normalize the equations (1), (3), (4) and (5), the following dimensionless parameters are introduced.

$$U_o = \frac{u_0}{\bar{u}} ,$$

$$U = \frac{u}{\bar{u}} ,$$

$$Y = \frac{y}{r_0} ,$$

$$D_{el} = \frac{\delta}{r_0} ,$$

$$X = \frac{x/D}{\frac{\rho \bar{u} D}{\mu}} = \frac{x/D}{Re_D} ,$$

$$P = \frac{p_0 - p}{\rho \bar{u}^2} .$$

Equations (1), (3), (4) and (5) become

$$\frac{U}{U_c} = 2\left(\frac{Y}{D_{el}}\right) - \left(\frac{Y}{D_{el}}\right)^2 , \tag{6}$$

$$D_{el} = 2 - \sqrt{4 - 6\left(1 - \frac{1}{U_c}\right)} , \tag{7}$$

$$X = \frac{1}{16}\left[\frac{58}{15}\eta - \frac{22}{5}\ln(1+\eta) - \frac{17}{15}\sqrt{4+2\eta-2\eta^2} - \frac{16}{5}\sqrt{\frac{4-2\eta}{1+\eta}} - \frac{37\sqrt{2}}{10}\sin^{-1}\left(\frac{2\eta-1}{3}\right) - \frac{37\sqrt{2}}{10}\sin^{-1}\left(\frac{1}{3}\right) + \frac{26}{3}\right] . \tag{8}$$

$$P = \frac{1}{2}\left[(\eta^2 - \eta_0^2) + 2(\eta - \eta_0)\right] . \tag{9}$$

where

$$\eta = U_c - 1 \; . \tag{10}$$

In order to use available subroutines, arcsine functions are changed to arctangent functions as follows:

$$\sin^{-1}\left(\frac{2\eta-1}{3}\right) = \tan^{-1}\left(\frac{2\eta-1}{2\sqrt{2+\eta-\eta^2}}\right) \; ,$$

$$\sin^{-1}\left(\frac{1}{3}\right) = \tan^{-1}\left(\frac{1}{2\sqrt{2}}\right) \; .$$

The computational procedure is

(i) Given a value of U_c, the center line velocity, then η is obtained from equation (10).

(ii) The values of the boundary layer thickness, D_{el}, the location from the entry, X, and the pressure drop, P, can be obtained from equations (7), (8) and (9), respectively.

(iii) The velocity distribution, U, at the corresponding section is obtained from equation (6).

The center line velocities (or core velocities) are $U_o = 1.0$ at the entry where $X = 0$ and $U_o = 2.0$ at the fully developed section. The mesh size for the calculation of the velocity profile and pressure drop is shown in Table 2.1.

A flow chart (Table 2.2) will be followed by a symbol table (Table 2.3) and FORTRAN program (Table 2.4). The computation is carried out by use of an IBM 1620 computer.

Table 2.1. Mesh sizes for the velocity profile and pressure drop in the entrance region

U_c	ΔU_c	ΔY	N^{+}
1.0005			
	.0005	$D_{el}/5$	5
1.01			
	.001	$D_{el}/5$	5
1.02			
	.005	$D_{el}/5$	5
1.07			
	.01	$D_{el}/5$	5
1.20			
	.05	$D_{el}/10$	10
2.0			
(fully developed)			

+ N = points within the boundary layer.

Table 2.2. Flow chart of Schiller's Method

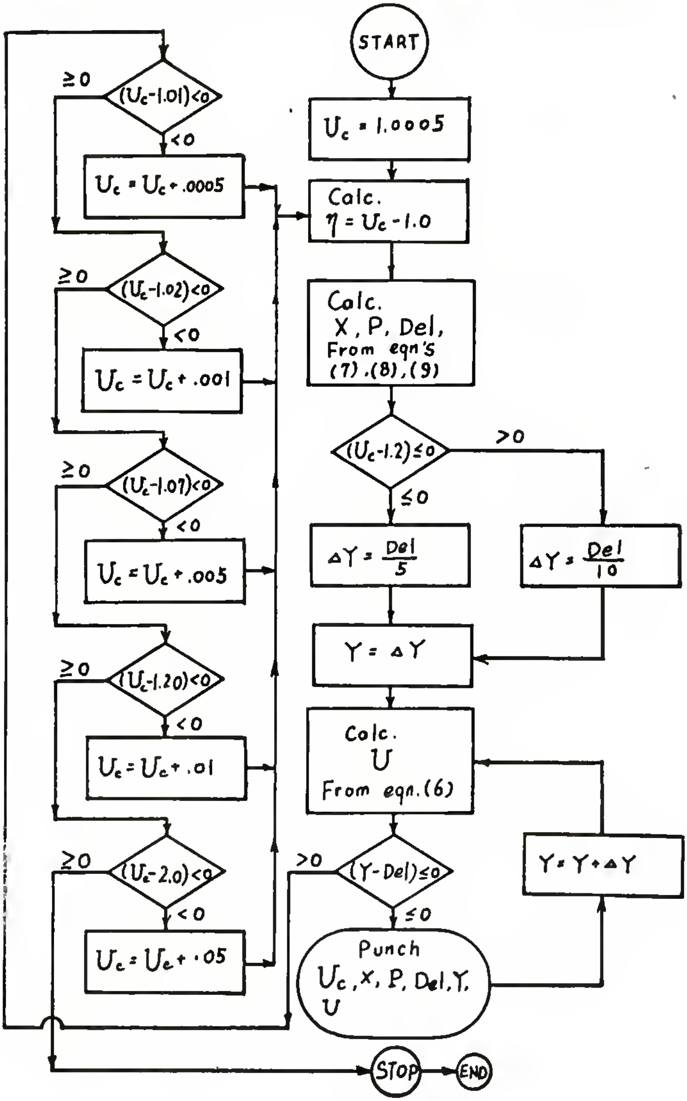

Table 2.3. Symbol Table

FORTRAN Symbol	Variables
DEL	D_{el}
DLTYR	ΔY
ET	η
P	P
S	$\sqrt{2}$
U	U
UC	U_c
XD	X
YR	Y

TABLE 2.4. FORTRAN PROGRAM FOR SCHILLER'S METHOD

```
C    C   SCHILLER,S METHOD
      1 FORMAT(/E12.5.F12.4, 4F12.5)
    100 FORMAT (48X, 2F12.5 )
        UC=1.0005
        S=1.4142135
      2 ET=UC-1.
        XD=1./16.*(58./15.*ET-22./5.*LOG(1.+ET))
        XD=XD-17./(16.*15.)*SQRT(4.+2.*ET-2.*ET*ET)
        XD=XD-1./5.*SQRT((4.-2.*ET)/(1.+ET))
        XD=XD-1./16.*3.7*S*ATAN((ET-.5)/SQRT(2.+ET-ET*ET))
        XD=XD-1./16.*(3.7*S*ATAN(1./(2.*S))-26./3.)
        P=(ET*ET+2.*ET)/2.
      3 DEL=2.-SQRT(-2.+6./UC)
        IF(UC-1.2) 4,4,5
      4 DLTYR=DEL/5.
        GO TO 41
      5 DLTYR=DEL/10.
     41 YR=DLTYR
      6 U=UC*(2.*(YR/DEL)-(YR/DEL)*(YR/DEL))
        IF(YR-DEL) 61, 61, 8
     61 IF(YR-DLTYR) 62,62,63
     62 PUNCH 1, UC,XD,P,DEL,YR,U
        GO TO 7
     63 PUNCH 100, YR,U
      7 YR=YR+DLTYR
        GO TO 6
      8 IF (UC-1.01) 14,10,10
     14 UC=UC+.0005
        GO TO 2
     10 IF(UC-1.02) 15,12,12
     15 UC=UC+.001
        GO TO 2
     12 IF (UC-1.07) 16,13,13
     16 UC=UC+.005
        GO TO 2
     13 IF(UC-1.20) 17,20,20
     17 UC=UC+.01
        GO TO 2
     20 IF(UC-2.0) 18.19,19
     18 UC=UC+.05
        GO TO 2
     19 STOP
        END
```

2.3. Results

Some numerical results are tabulated in Table 2.5. The developing velocity profile is shown in Fig. 2.3. The pressure drops in the entrance region are plotted in Fig. 2.4.

```
TABLE 2.5.  SAMPLE NUMERICAL RESULTS FOR SCHILLER'S METHOD


   UC              XD           P              DEL             YR              U

.10500E+01  0.5057E-04 0.51250E-01 0.72752E-01 0.14550E-01 0.37800
                                                .29101E-01 0.67200
                                                .43651E-01 0.88200
                                                .58201E-01 0.10080E+01
                                                .72752E-01 0.10500E+01

.11000E+01  0.2146E-03 0.10500     0.14136     0.28272E-01 0.39600
                                                .56544E-01 0.70400
                                                .84816E-01 0.92400
                                                .11309     0.10560E+01
                                                .14136     0.11000E+01

.12000E+01  0.9393E-03 0.22000     0.26795     0.53590E-01 0.43200
                                                .10718     0.76800
                                                .16077     0.10080E+01
                                                .21436     0.11520E+01
                                                .26795     0.12000E+01

.13000E+01  0.2251E-02 0.34500     0.38279     0.38279E-01 0.24700
                                                .76557E-01 0.46800
                                                .11484     0.66300
                                                .15311     0.83200
                                                .19139     0.97500
                                                .22967     0.10920E+01
                                                .26795     0.11830E+01
                                                .30623     0.12480E+01
                                                .34451     0.12870E+01
                                                .38279     0.13000E+01

.14000E+01  0.4185E-02 0.48000     0.48814     0.48814E-01 0.26600
                                                .97628E-01 0.50400
                                                .14644     0.71400
                                                .19526     0.89600
                                                .24407     0.10500E+01
                                                .29289     0.11760E+01
                                                .34170     0.12740E+01
                                                .39051     0.13440E+01
                                                .43933     0.13860E+01
                                                .48814     0.14000E+01

.15000E+01  0.6755E-02 0.62500     0.58579     0.58579E-01 0.28500
                                                .11716     0.54000
                                                .17574     0.76500
                                                .23431     0.96000
                                                .29289     0.11250E+01
                                                .35147     0.12600E+01
                                                .41005     0.13650E+01
                                                .46863     0.14400E+01
                                                .52721     0.14850E+01
                                                .58579     0.15000E+01
```

```
    UC           XD           P               DEL              YR           U

.16000E+01  0.9957E-02 0.78000        0.67712         0.67712E-01 0.30400
                                                       .13542      0.57600
                                                       .20314      0.61600
                                                       .27085      0.10240E+01
                                                       .33856      0.12000E+01
                                                       .40627      0.13440E+01
                                                       .47399      0.14560E+01
                                                       .54170      0.15360E+01
                                                       .60941      0.15840E+01
                                                       .67712      0.16000E+01

.17000E+01  0.1378E-01 0.94500        0.76331         0.76331E-01 0.32300
                                                       .15266      0.61200
                                                       .22899      0.86700
                                                       .30532      0.10880E+01
                                                       .38165      0.12750E+01
                                                       .45798      0.14280E+01
                                                       .53431      0.15470E+01
                                                       .61065      0.16320E+01
                                                       .68698      0.16830E+01
                                                       .76331      0.17000E+01

.18000E+01  0.1826E-01 0.11200E+01 0.84530         0.84530E-01 0.34200
                                                       .16906      0.64800
                                                       .25359      0.91800
                                                       .33812      0.11520E+01
                                                       .42265      0.13500E+01
                                                       .50718      0.15120E+01
                                                       .59171      0.16380E+01
                                                       .67624      0.17280E+01
                                                       .76077      0.17820E+01
                                                       .84530      0.18000E+01

.19000E+01  0.2321E-01 0.13050E+01 0.92394         0.92394E-01 0.36100
                                                       .18479      0.68400
                                                       .27718      0.96900
                                                       .36958      0.12160E+01
                                                       .46197      0.14250E+01
                                                       .55437      0.15960E+01
                                                       .64676      0.17290E+01
                                                       .73916      0.18240E+01
                                                       .83155      0.18810E+01
                                                       .92394      0.19000E+01

.20000E+01  0.2877E-01 0.15000E+01 0.10000E+01 0.10000     0.38000
                                                       .20000      0.72000
                                                       .30000      0.10200E+01
                                                       .40000      0.12800E+01
                                                       .50000      0.15000E+01
                                                       .60000      0.16800E+01
                                                       .70000      0.18200E+01
                                                       .80000      0.19200E+01
                                                       .90000      0.19800E+01
                                                       .10000E+01 0.20000E+01
```

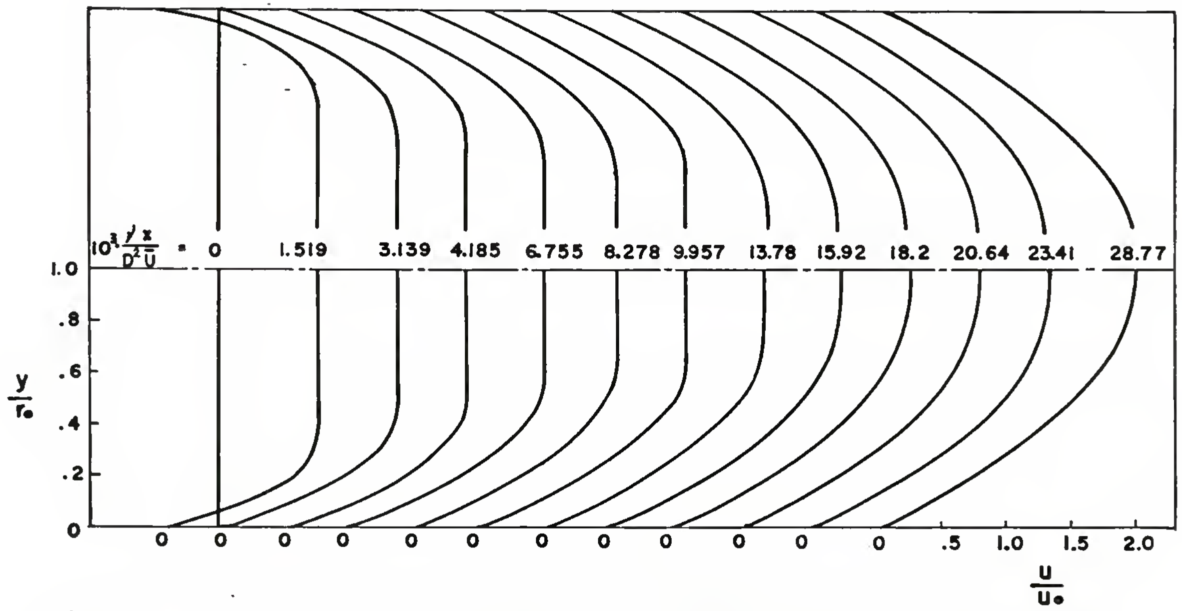

Fig. 2.3. Velocity distribution for laminar flow in the inlet section of a circular tube.

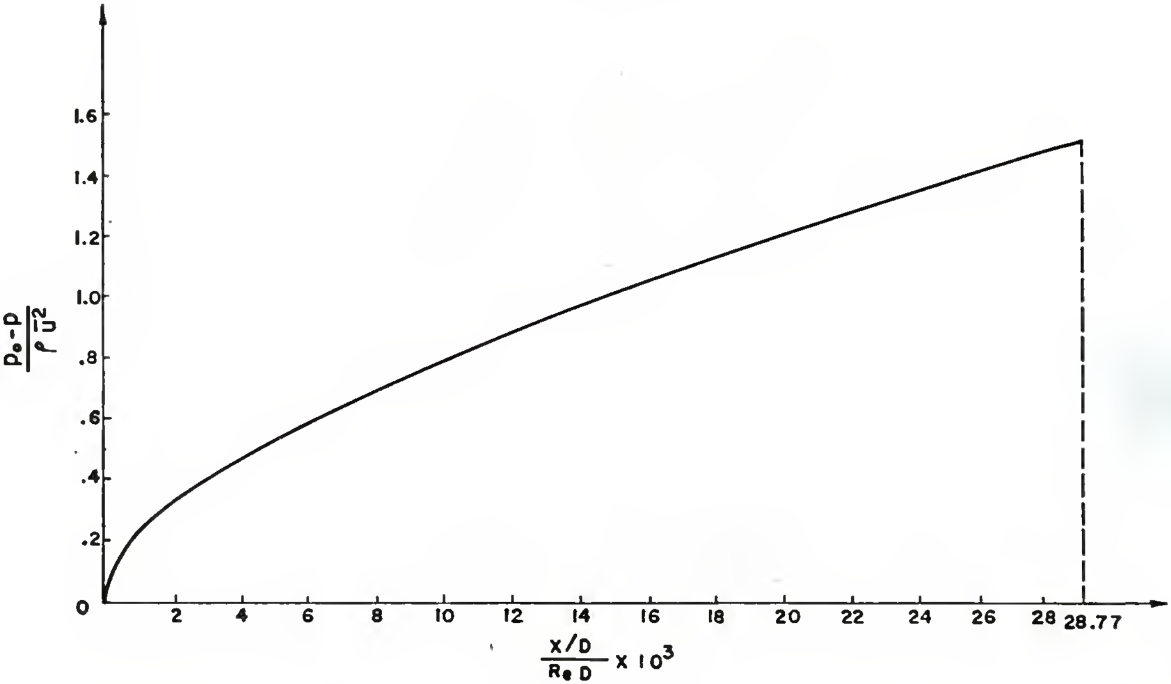

Fig. 2.4. Pressure drops for laminar flow in the entrance region of a circular tube.

2.4. Sample Calculation with Dimensions

As soon as the dimensionless results are obtained, the values with any dimension can be calculated.

For example, we have three different kinds of fluids, air, water, and lubricating oil, with their properties listed in Table 2.6. The diameter of the tube and the average velocity are assumed to be the same for all three fluids. Assuming that $D = 1/4$ ft, $\bar{u} = 1/10$ ft/sec, we try to compare the entrance length and pressure drop from the entry to the place where the fluid is fully developed. Here, the assumption is made that the fluids are incompressible.

For air:

$$Re_D = \frac{\bar{u}D}{\nu} = \frac{1}{10 \cdot 4 \cdot 1.460} \cdot 10^4 = 1.712 \cdot 10^2$$

Using the output data that $X = .02877$, and $P = 1.5$, we obtain

$$x_e = X \cdot Re_D \cdot D = .02877 \cdot 1.712 \cdot 10^2 \cdot \frac{1}{4} = 1.231 \text{ ft} ,$$

$$x_e/D = 1.231/(1/4) = 4.924 ,$$

$$\Delta p = p_0 - p_e = P \cdot \rho \bar{u}^2$$

$$= 1.5 \cdot (.00237) \cdot \left(\frac{1}{10}\right)^2 \cdot \frac{1}{144}$$

$$= 2.464 \cdot 10^{-7} \text{ psia}$$

The calculations for water and oil proceed in the same way, and the results are shown in Table 2.6.

Table 2.6. Fluid properties and calculation results

Fluids	°F	D(ft)	$\bar{u}(\frac{ft}{sec})$	$\rho(\frac{slug}{ft^3})$	$\mu(\frac{lb\text{-}sec}{ft^2})$	$\nu(\frac{ft^2}{sec})$	Re_D	x_e(ft)	Δp(psia)	x_e/D
Air	60	1/4	1/10	.00237	3.78×10^{-7}	1.46×10^{-4}	1.712×10^{2}	1.231	2.464×10^{-7}	4.92
Water	60	1/4	1/10	1.938	2.35×10^{-5}	1.217×10^{-5}	2.054×10^{3}	14.77	2.015×10^{-4}	59.1
White Mineral Oil (SAE30)	60	1/4	1/10	1.718	7.73×10^{-3}	4.50×10^{-3}	5.555	.0399	1.786×10^{-4}	.160

REFERENCES

1. Schiller, L., "Die Entwicklung der laminaren Geschwindigkeitsverteilung und ihre Bedeutung für Zahigkeitmessungen", ZAMM, 2, 96-106, 1922.

2. Li, K. C., "Analytical and Numerical Solutions of Some Entrance Region Flow Problems", M.S. Report, Mech. Engg., Kansas State Univ., Jan. 1966.

3. Schlichting, H., "Boundary Layer Theory", p. 35, p. 168, McGraw-Hill, New York, 4th ed., 1960.

CHAPTER 3. LANGHAAR'S LINEARIZING APPROXIMATE METHOD

3.1. Description of the Method [1]

Because of the nonlinear convective terms involved in the boundary layer equations, it is difficult to obtain an exact analytical solution. By means of a linearizing approximation, Langhaar assumed that the convective terms in the boundary layer equation in the axial direction, x, (Fig. 2.1) are equal to the product of the kinematic viscosity ν, the axial velocity u and a parameter β which is considered to be a function of x only.

Langhaar's assumption can be written as

$$u \frac{\partial u}{\partial x} + v \frac{\partial u}{\partial y} + w \frac{\partial u}{\partial z} = \nu \beta^2 u \tag{1}$$

and gives rise to the following linearized form of the boundary layer equation

$$\nu \beta^2 u = g_x - \frac{1}{\rho} \frac{dp}{dx} + \nu \left(\frac{\partial^2 u}{\partial y^2} + \frac{\partial^2 u}{\partial z^2} \right) . \tag{2}$$

In order to solve the problem for a flow in a circular tube, equation (2) is transformed into a cylindrical coordinate form as

$$\frac{d^2 u}{dr^2} + \frac{1}{r} \frac{du}{dr} - \beta^2 u = \alpha \tag{3}$$

where

$$\alpha = - \frac{1}{\nu} \left(g_x - \frac{1}{\rho} \frac{dp}{dx} \right)$$

which is a function of x alone.

The solution of equation (3) is expressed in terms of modified Bessel functions as

$$U = \frac{u}{\bar{u}} = \frac{I_0(\gamma) - I_0(\gamma \frac{r}{r_0})}{I_2(\gamma)} \tag{4}$$

where $\gamma = \beta r_0$, r_0 is the radius of the tube.

Equation (4) will define the velocity profiles in the entrance region if the relation between γ and x is known.

When $\beta = 0$, (that is, $\gamma = 0$), the acceleration terms are zero. The solution then assumes the form of a fully developed parabolic profile. When $\beta \longrightarrow \infty$, (that is, $\gamma \longrightarrow \infty$) the solution assumes a uniform profile at the entry. Therefore, the solution provides a smooth transition from the entry where $\gamma \longrightarrow \infty$ to the fully developed section where $\gamma = 0$.

For determining the relation between γ and x, the momentum integral equation is used. Integrating the boundary layer equation in cylindrical coordinates over the cross section, we obtain

$$2 \frac{d}{dx} \int_0^{r_0} u^2 r dr = g_x r_0^2 - \frac{1}{\rho} \frac{dp}{dx} r_0^2 + 2 \nu \int_0^{r_0} \left(\frac{\partial^2 u}{\partial r^2} + \frac{1}{r} \frac{\partial u}{\partial r}\right) r dr. \tag{5}$$

After the substitution of (4) and simplification, we obtain the following relations:

$$X = \int_Z^{1/2} Y dZ \tag{6}$$

where

$$X = \frac{x}{r_0 \ Re_r} \tag{7}$$

$$Y = \frac{I_2(\gamma)}{2\gamma I_1(\gamma) - \gamma^2} \tag{8}$$

and

$$Z = \frac{4I_0(\gamma)I_2(\gamma) - [I_0(\gamma) - 1]^2 - 2I_1^2(\gamma)}{2I_2^2(\gamma)} . \tag{9}$$

It can be shown that the limits for variables Z and Y are:

$$Z \longrightarrow \frac{1}{2}, \qquad Y \longrightarrow 0 \qquad \text{as} \qquad \gamma \longrightarrow \infty$$

$$Z \longrightarrow -\frac{2}{3}, \qquad Y \longrightarrow \infty \qquad \text{as} \qquad \gamma \longrightarrow 0 .$$

Equation (6) provides a relation between x and γ. The integration can be carried out numerically as will be shown later on.

The entrance length is defined as the distance from the entry to a section where the center line velocity is 99 per cent of the fully developed one; that is,

$$u_0 = 0.99\,(u_0)_{F.D.}$$

or

$$\frac{u_0}{\bar{u}} = 0.99\,\frac{(u_0)_{F.D.}}{\bar{u}} .$$

Since

$$\frac{(u_0)_{F.D.}}{\bar{u}} = 2$$

hence

$$U_0 = \frac{u_0}{\bar{u}} = 0.99 \times 2 = 1.98 .$$

This is equivalent to saying that the entrance length is the distance from the entry to a section where the dimensionless center line velocity, U_0, is equal to 1.98. The values of U_0 at various sections can be obtained from (4) with $\frac{r}{r_0} = 0$; that is,

$$U_0 = \frac{u_0}{\bar{u}} = \frac{I_0(\gamma) - 1}{I_2(\gamma)} . \tag{10}$$

Hence, when $U_0 = 1.98$, the corresponding value of γ (and therefore the value of x) can be determined.

In calculating the pressure drop in the entrance region, Langhaar applied the mechanical energy balance instead of using the Bernoulli equation because in the downstream part of the entrance region where the velocity approaches the fully developed one, the Bernoulli equation ceases to be applicable. The energy loss due to viscous dissipation was considered. Equating the work of pressure force and frictional force to the change in kinetic energy gives the energy equation

$$\bar{u}A(p_0 - p) = \mu \int_0^x dx \int_A \left(\frac{\partial u}{\partial r}\right)^2 dA + \frac{1}{2} \rho \int_A (u^3 - \bar{u}^3) dA \tag{11}$$

where A is the cross-sectional area of the tube and μ is the viscosity of the fluid.

Substituting (4) into (11) and simplifying, gives the total pressure drop between a supply reservoir and the section x in the entrance region:

$$P = \frac{p_\infty - p}{\frac{1}{2}\cdot \rho \bar{u}^2} = 1+2\int_0^X \frac{\gamma^2}{I_2^2}(I_1^2 - I_0 I_2)\,dX + 2\int_0^1 (U^3-1)R\,dR \qquad (12)$$

where

$$U = \frac{u}{\bar{u}}, \qquad R = \frac{r}{r_0}.$$

Equation (12) can be carried out numerically and will be shown in the later part of this chapter. Hence the pressure drops in the entrance region are defined.

The detailed derivation of the equations is given in Li's report [2].

3.2. Computational Procedures

The available modified Bessel function data for arguments from 0 to 85 [3] are used in this computation. The computation for entrance length, velocity distribution and pressure distribution will be given separately by three different FORTRAN programs.

(1) Entrance Length

The relationship between the length in the entrance region, X, and the parameter, γ, is given by equation (6). The function $X(\gamma)$ is represented by the area under a curve (see Fig. 3.1) represented by $Y(\gamma)$, which is a function of γ as shown in equation (8), in the interval of $Z(\gamma)$, $(Z, \frac{1}{2})$, which is also a function of γ as shown in equation (9). By assigning a set of values for γ, a set of the corresponding values for $Z(\gamma)$, and $Y(\gamma)$ can be obtained from equations (9) and (8) respectively. Then the corresponding values of $X(\gamma)$ are obtained by numerical integration of equation (6).

The set of values assigned to γ are chosen from 100 to 0.1 and the intervals between each γ is shown in Table 3.1.

The values of $I_0(\gamma)$ and $I_1(\gamma)$ for $\gamma = 100, 95, 90$ are obtained from the following polynomial approximate relations [6].

$$\begin{aligned}\gamma^{\frac{1}{2}} e^{-\gamma} I_0(\gamma) &= 3.9894228 + 0.1328592t^{-1} + .00225319t^{-2} \\ &\quad - .00157565t^{-3} + .00916281t^{-4} - .02057706t^{-5}\end{aligned}$$

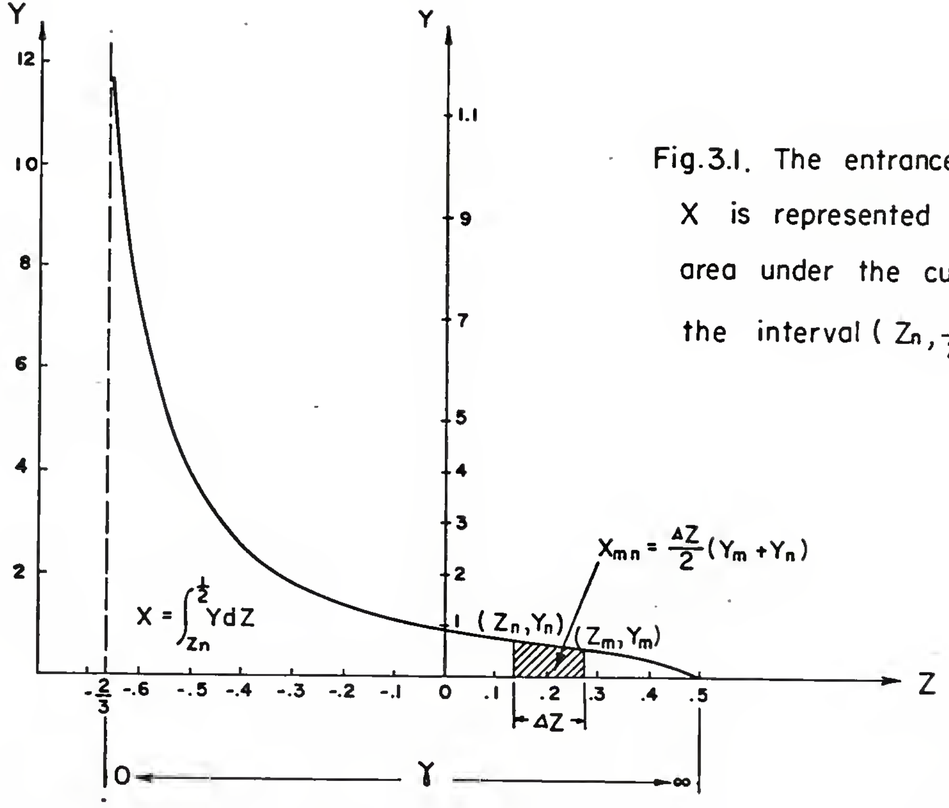

Fig. 3.1. The entrance length X is represented by the area under the curve in the interval $(Z_n, \frac{1}{2})$.

Table 3.1. Selected interval between each γ

γ	$\Delta\gamma$	N*
100		
	5.0	15
30		
	1.0	15
15		
	0.5	16
7.0		
	0.2	20
3.0		
	0.1	29
0.1		

N*: Points within the interval.

$$+ .02635537t^{-6} - .01647633t^{-7}$$

$$+ .00392377t^{-8} + \epsilon . \qquad (13)$$

where

$$3.75 \le \gamma \le \infty , \qquad t = \frac{\gamma}{3.75}$$

$$|\epsilon| < 1.9 \times 10^{-7} .$$

and

$$\gamma^{\frac{1}{2}} e^{-\gamma} I_1(\gamma) = .39894228 - .03988024t^{-1} - .00362018t^{-2}$$

$$+ .00163801t^{-3} - .01031555t^{-4} + .02282967t^{-5}$$

$$- .02895312t^{-6} + .01787654t^{-7}$$

$$- .00420059t^{-8} + \epsilon . \qquad (14)$$

where

$$3.75 \le \gamma \le \infty , \qquad t = \frac{\gamma}{3.75}$$

$$|\epsilon| < 2.2 \times 10^{-7} .$$

In the computation, the values of $I_0(\gamma)$ and $I_1(\gamma)$ for the corresponding values of γ are given as the input data in the FORTRAN program and the value of $I_2(\gamma)$ corresponding to each value of γ is computed by the following relation [4]:

$$I_2(\gamma) = - \frac{2}{\gamma} I_1(\gamma) + I_0(\gamma) \qquad (15)$$

The integration of equation (6) proceeds from the large value of γ to the small one and the trapezoidal method [5] is applied in the integration (see Fig. 3.1). The center line velocity corresponding to each entrance length is also computed from equation (10).

A flow chart (Table 3.2) will be followed by a symbol table (Table 3.3) and FORTRAN program (Table 3.4). The whole oomputation is carried out by an IBM 1620 computer and some numerical results are tabulated in Table 3.5.

Table 3.2. Flow chart of Langharr's Method — entrance length

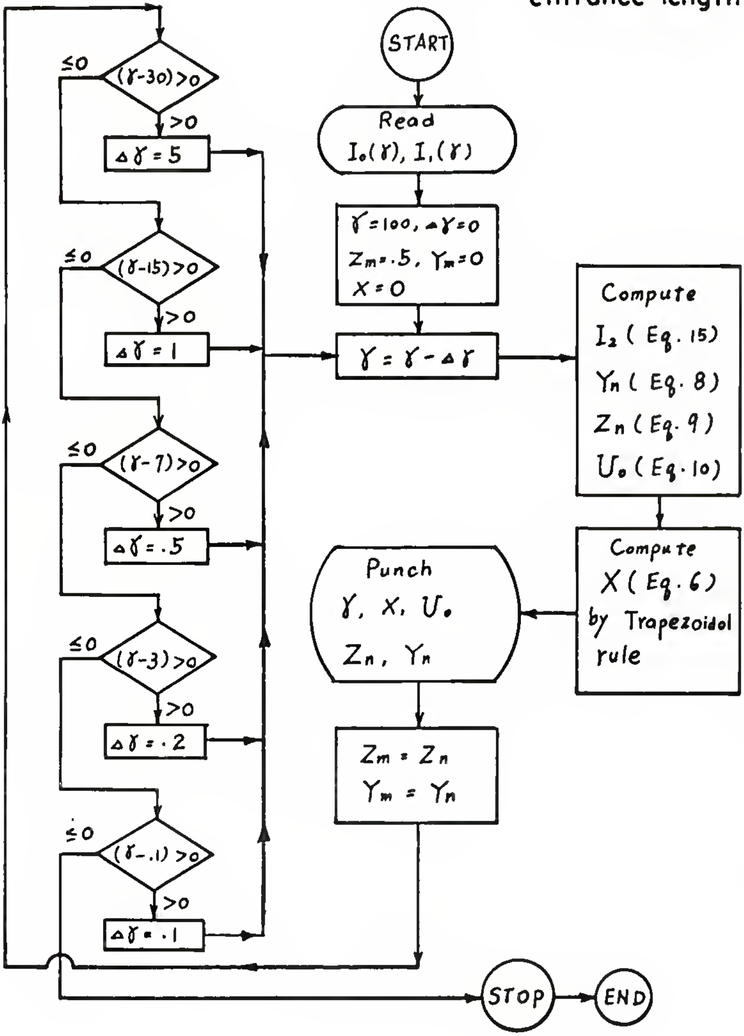

Table 3.3. Symbol Table

FORTRAN Symbol	Variables
BIO(N)	$I_0(\gamma)$
BI1(N)	$I_1(\gamma)$
GAMA	γ
ZM	Z_m
YM	Y_m
DELTG	$\Delta\ \gamma$
BI2N	$I_2(\gamma)$
ZN	Z_n
YN	Y_n
DZ	$\Delta\ Z$
X	X
UO	U_0

TABLE 3.4. FORTRAN PROGRAM FOR LANGHAAR'S METHOD
---ENTRANCE LENGTH

```
C  C  LANGHAAR,S METHOD -----ENTRANCE LENGTH
 111 FORMAT(3E12.4)
  10 FORMAT(6F12.4)
  11 FORMAT(I2,F5.1, 2E11.4, 4E10.3)
     DIMENSION BIO(100), BI1(100)
     READ 111,(BIO(N),N=1,3)
     READ 10,(BIO(N),N=4,95)
     READ 111,(BI1(N),N=1,3)
     READ  10,(BI1(N),N=4,95)
     N=0
     GAMA=100.
     ZM=.5
     YM=.0
     X=.0
     DELTG=.0
   2 GAMA=GAMA-DELTG
     N=N+1
     BI2N=-2.*BI1(N)/GAMA+BIO(N)
     ZN=2.*BIO(N)/BI2N-((BIO(N)-1.)/BI2N)*((BIO(N)-1.)/BI2N)/2.
     ZN=ZN-(BI1(N)/BI2N)*(BI1(N)/BI2N)
     YN=BI2N/(2.*GAMA*BI1(N)-GAMA*GAMA)
     DZ=ZM-ZN
  20 X=X+(YM+YN)*DZ/2.
     U0=BIO(N)/BI2N-1./BI2N
     PUNCH 11, N,GAMA,X,U0,BIO(N),BI1(N),ZN,YN
     ZM=ZN
     YM=YN
     IF(GAMA-30.)31,31,3
   3 DELTG=5.
     GO TO 2
  31 IF(GAMA-15.)41,41,4
   4 DELTG=1.
     GO TO 2
  41 IF(GAMA-7.)51,51,5
   5 DELTG=.5
     GO TO 2
  51 IF(GAMA-3.)61,61,6
   6 DELTG=.2
     GO TO 2
  61 IF(GAMA-.1)71,71,7
   7 DELTG=.1
     GO TO 2
  71 STOP
     END
```

TABLE 3.5. NUMERICAL RESULTS OF LANGHAAR'S METHOD---ENTRANCE LENGTH

N	GAMA	X	UO	BIO(N)	BI1(N)	ZN	YN
1	100.0	0.2772E-04	0.1020E+01	0.107E+43	0.107E+43	0.489	0.492E-02
2	95.0	0.2570E-04	0.1021E+01	0.742E+40	0.738E+40	0.489	0.518E-02
3	90.0	0.2960E-04	0.1023E+01	0.514E+38	0.511E+38	0.488	0.546E-02
4	85.0	0.3463E-04	0.1024E+01	0.356E+36	0.354E+36	0.488	0.578E-02
5	80.0	0.4213E-04	0.1025E+01	0.248E+34	0.246E+34	0.486	0.613E-02
6	75.0	0.4161E-04	0.1027E+01	0.172E+32	0.171E+32	0.486	0.654E-02
7	70.0	0.4834E-04	0.1029E+01	0.120E+30	0.119E+30	0.485	0.699E-02
8	65.0	0.6229E-04	0.1031E+01	0.840E+27	0.834E+27	0.483	0.752E-02
9	60.0	0.7517E-04	0.1034E+01	0.589E+25	0.585E+25	0.482	0.813E-02
10	55.0	0.8892E-04	0.1037E+01	0.415E+23	0.411E+23	0.480	0.884E-02
11	50.0	0.1061E-03	0.1041E+01	0.293E+21	0.290E+21	0.478	0.970E-02
12	45.0	0.1410E-03	0.1046E+01	0.208E+19	0.206E+19	0.475	0.107E-01
13	40.0	0.1900E-03	0.1052E+01	0.149E+17	0.147E+17	0.471	0.120E-01
14	35.0	0.2473E-03	0.1060E+01	0.107E+15	0.106E+15	0.466	0.137E-01
15	30.0	0.3253E-03	0.1070E+01	0.782E+12	0.769E+12	0.461	0.158E-01
16	29.0	0.3522E-03	0.1073E+01	0.293E+12	0.287E+12	0.459	0.164E-01
17	28.0	0.4088E-03	0.1075E+01	0.110E+12	0.108E+12	0.456	0.169E-01
18	27.0	0.4110E-03	0.1078E+01	0.410E+11	0.403E+11	0.456	0.175E-01
19	26.0	0.4471E-03	0.1082E+01	0.154E+11	0.151E+11	0.454	0.181E-01
20	25.0	0.4892E-03	0.1085E+01	0.578E+10	0.566E+10	0.451	0.188E-01
21	24.0	0.5317E-03	0.1089E+01	0.217E+10	0.212E+10	0.449	0.195E-01
22	23.0	0.5942E-03	0.1093E+01	0.815E+09	0.797E+09	0.446	0.203E-01
23	22.0	0.6475E-03	0.1097E+01	0.307E+09	0.300E+09	0.443	0.212E-01
24	21.0	0.7210E-03	0.1102E+01	0.116E+09	0.113E+09	0.440	0.221E-01
25	20.0	0.8051E-03	0.1108E+01	0.436E+08	0.425E+08	0.436	0.232E-01
26	19.0	0.9111E-03	0.1114E+01	0.165E+08	0.160E+08	0.432	0.243E-01
27	18.0	0.1039E-02	0.1121E+01	0.622E+07	0.604E+07	0.427	0.255E-01
28	17.0	0.1192E-02	0.1129E+01	0.236E+07	0.229E+07	0.421	0.269E-01
29	16.0	0.1366E-02	0.1138E+01	0.893E+06	0.865E+06	0.415	0.284E-01
30	15.0	0.1585E-02	0.1148E+01	0.340E+06	0.328E+06	0.407	0.301E-01
31	14.5	0.1694E-02	0.1153E+01	0.210E+06	0.202E+06	0.403	0.310E-01
32	14.0	0.1865E-02	0.1160E+01	0.129E+06	0.125E+06	0.398	0.320E-01
33	13.5	0.2014E-02	0.1166E+01	0.800E+05	0.769E+05	0.393	0.330E-01
34	13.0	0.2217E-02	0.1173E+01	0.494E+05	0.475E+05	0.387	0.341E-01
35	12.5	0.2435E-02	0.1181E+01	0.306E+05	0.294E+05	0.381	0.353E-01
36	12.0	0.2669E-02	0.1190E+01	0.190E+05	0.181E+05	0.375	0.366E-01
37	11.5	0.2905E-02	0.1199E+01	0.118E+05	0.112E+05	0.368	0.380E-01
38	11.0	0.3324E-02	0.1210E+01	0.729E+04	0.695E+04	0.357	0.394E-01
39	10.5	0.3718E-02	0.1221E+01	0.453E+04	0.431E+04	0.348	0.410E-01
40	10.0	0.4165E-02	0.1234E+01	0.282E+04	0.267E+04	0.337	0.428E-01

```
  N GAMA       X            UO          BIO(N)     BI1(N)       ZN           YN

 41   9.5 0.4737E-02 0.1248E+01 0.175E+04 0.166E+04 0.324         0.447E-01
 42   9.0 0.5363E-02 0.1264E+01 0.109E+04 0.103E+04 0.310         0.468E-01
 43   8.5 0.6208E-02 0.1282E+01 0.683E+03 0.642E+03 0.293         0.491E-01
 44   8.0 0.7214E-02 0.1302E+01 0.428E+03 0.400E+03 0.273         0.517E-01
 45   7.5 0.8425E-02 0.1325E+01 0.268E+03 0.250E+03 0.250         0.547E-01

 46   7.0 0.9903E-02 0.1351E+01 0.169E+03 0.156E+03 0.224         0.581E-01
 47   6.8 0.1079E-01 0.1363E+01 0.140E+03 0.129E+03 0.209         0.595E-01
 48   6.6 0.1153E-01 0.1375E+01 0.117E+03 0.107E+03 0.196         0.612E-01
 49   6.4 0.1233E-01 0.1388E+01 0.970E+02 0.890E+02 0.183         0.629E-01
 50   6.2 0.1327E-01 0.1401E+01 0.807E+02 0.739E+02 0.169         0.648E-01

 51   6.0 0.1431E-01 0.1416E+01 0.672E+02 0.613E+02 0.153         0.668E-01
 52   5.8 0.1546E-01 0.1431E+01 0.560E+02 0.510E+02 0.136         0.690E-01
 53   5.6 0.1672E-01 0.1446E+01 0.467E+02 0.423E+02 0.118         0.714E-01
 54   5.4 0.1809E-01 0.1463E+01 0.390E+02 0.352E+02 0.992E-01 0.741E-01
 55   5.2 0.1967E-01 0.1481E+01 0.326E+02 0.293E+02 0.784E-01 0.770E-01

 56   5.0 0.2149E-01 0.1499E+01 0.272E+02 0.243E+02 0.552E-01 0.801E-01
 57   4.8 0.2334E-01 0.1518E+01 0.228E+02 0.203E+02 0.326E-01 0.838E-01
 58   4.6 0.2546E-01 0.1538E+01 0.191E+02 0.169E+02 0.793E-02 0.878E-01
 59   4.4 0.2802E-01 0.1560E+01 0.160E+02 0.141E+02-0.206E-01 0.923E-01
 60   4.2 0.3086E-01 0.1582E+01 0.134E+02 0.117E+02-0.505E-01 0.974E-01

 61   4.0 0.3354E-01 0.1604E+01 0.113E+02 0.976E+01-0.771E-01 0.103
 62   3.8 0.3672E-01 0.1628E+01 0.952E+01 0.814E+01-0.107       0.110
 63   3.6 0.4052E-01 0.1652E+01 0.803E+01 0.679E+01-0.140       0.118
 64   3.4 0.4467E-01 0.1677E+01 0.679E+01 0.567E+01-0.174       0.128
 65   3.2 0.4944E-01 0.1703E+01 0.575E+01 0.473E+01-0.210       0.139

 66   3.0 0.5458E-01 0.1728E+01 0.488E+01 0.395E+01-0.245       0.153
 67   2.9 0.5787E-01 0.1742E+01 0.450E+01 0.361E+01-0.266       0.160
 68   2.8 0.6098E-01 0.1755E+01 0.416E+01 0.330E+01-0.285       0.169
 69   2.7 0.6388E-01 0.1767E+01 0.384E+01 0.302E+01-0.301       0.179
 70   2.6 0.6753E-01 0.1781E+01 0.355E+01 0.276E+01-0.321       0.190

 71   2.5 0.7175E-01 0.1794E+01 0.329E+01 0.252E+01-0.343       0.201
 72   2.4 0.7562E-01 0.1807E+01 0.305E+01 0.230E+01-0.361       0.215
 73   2.3 0.7969E-01 0.1820E+01 0.283E+01 0.210E+01-0.380       0.231
 74   2.2 0.8446E-01 0.1832E+01 0.263E+01 0.191E+01-0.400       0.248
 75   2.1 0.8823E-01 0.1844E+01 0.245E+01 0.175E+01-0.414       0.269

 76   2.0 0.9530E-01 0.1858E+01 0.228E+01 0.159E+01-0.440       0.291
 77   1.9 0.9776E-01 0.1868E+01 0.213E+01 0.145E+01-0.448       0.319
 78   1.8 0.1029      0.1880E+01 0.199E+01 0.132E+01-0.463       0.351
 79   1.7 0.1092      0.1891E+01 0.186E+01 0.120E+01-0.480       0.388
 80   1.6 0.1249      0.1905E+01 0.175E+01 0.109E+01-0.518       0.432
 N GAMA      X              UO         BIO(N)     BI1(N)        ZN          YN

81   1.5 0.1258       0.1914E+01 0.165E+01 0.982      -0.520      0.486
82   1.4 0.1467       0.1926E+01 0.155E+01 0.886      -0.560      0.551
83   1.3 0.1529       0.1935E+01 0.147E+01 0.797      -0.571      0.633
84   1.2 0.1433       0.1942E+01 0.139E+01 0.715      -0.557      0.737
85   1.1 0.1832       0.1953E+01 0.133E+01 0.638      -0.607      0.867

86   1.0 0.2005       0.1962E+01 0.127E+01 0.565      -0.625      0.104E 01
87    .9 0.1653       0.1966E+01 0.121E+01 0.497      -0.594      0.128E+01
88    .8 0.1868E-01 0.1971E+01 0.117E+01 0.433      -0.493      0.161E 01
89    .7 0.6694       0.1986E+01 0.113E+01 0.372      -0.847      0.207E+01
90    .6 0.2484       0.1986E+01 0.109E+01 0.314      -0.674      0.282E+01

91    .5 0.3954E+01 0.2006E+01 0.106E+01 0.258      -0.177E+01 0.397E+01
92    .4 0.5358E+01 0.2000E+01 0.104E+01 0.204      -0.204E+01 0.625E+01
93    .3-0.5119E+02 0.1971E+01 0.102E+01 0.152       0.435E+01 0.114E+02
94    .2 0.6476E+02 0.2000E+01 0.101E+01 0.101      -0.201E+01 0.250E+02
95    .1-0.2983E+05 0.1667E+01 0.100E+01 0.501E-01  0.340E+03 0.150E 03
```

(2) Velocity Distribution

Equation (4)

$$U = \frac{u}{\bar{u}} = \frac{I_0(\gamma) - I_0(\gamma \frac{r}{r_0})}{I_2(\gamma)} \qquad (4)$$

represents the velocity distribution at any value of γ in the entrance region. As shown in the previous article γ represents a corresponding value of x, the distance from the entry. The velocity distribution is assumed to be symmetric with respect to the center line. The values of the velocity at eleven points across the half circular tube, ($\frac{r}{r_0}$ = 1.0, 0.9,...., 0.1, 0) at a given value of γ are computed from equation (4). Table 3.6 shows the values of γ and $\gamma \frac{r}{r_0}$, where the velocity is computed.

A flow chart (Table 3.7) for this computation is followed by a symbol table (Table 3.8) and FORTRAN program (Table 3.9). The computation is also carried out by an IBM 1620 computer and some numerical results are tabulated in Table 3.10 and the velocity distribution for each location in the entrance region is plotted as shown in Fig. 3.2.

Table 3.6. Assigned values of γ and $\frac{r}{r_0}$ in computing the velocity distribution

γ for I_0 and I_1	$\Delta\gamma$	$\gamma\frac{r}{r_0}$ for I_0 γ $\frac{r}{r_0}$	40	20	15	8	6	5	4	3	2	1	0
40		1.0	40	20	15	8	6	5	4	3	2	1	0
	20	.9	36	18	13.5	7.2	5.4	4.5	3.6	2.7	1.8	.9	0
20		.8	32	16	12	6.4	4.8	4.0	3.2	2.4	1.6	.8	0
	5	.7	28	14	10.5	5.6	4.2	3.5	2.8	2.1	1.4	.7	0
15		.6	24	12	9.0	4.8	3.6	3.0	2.4	1.8	1.2	.6	0
	7	.5	20	10	7.5	4.0	3.0	2.5	2.0	1.5	1.0	.5	0
8		.4	16	8	6.0	3.2	2.4	2.0	1.6	1.2	.8	.4	0
	2	.3	12	6	4.5	2.4	1.8	1.5	1.2	.9	.6	.3	0
6		.2	8	4	3.0	1.6	1.2	1.0	.8	.6	.4	.2	0
	1	.1	4	2	1.5	.8	.6	.5	.4	.3	.2	.1	0
0		0.0	0	0	0	0	0	0	0	0	0	0	0

Table 3.7 Flow chart of Langharr's Method — velocity distribution

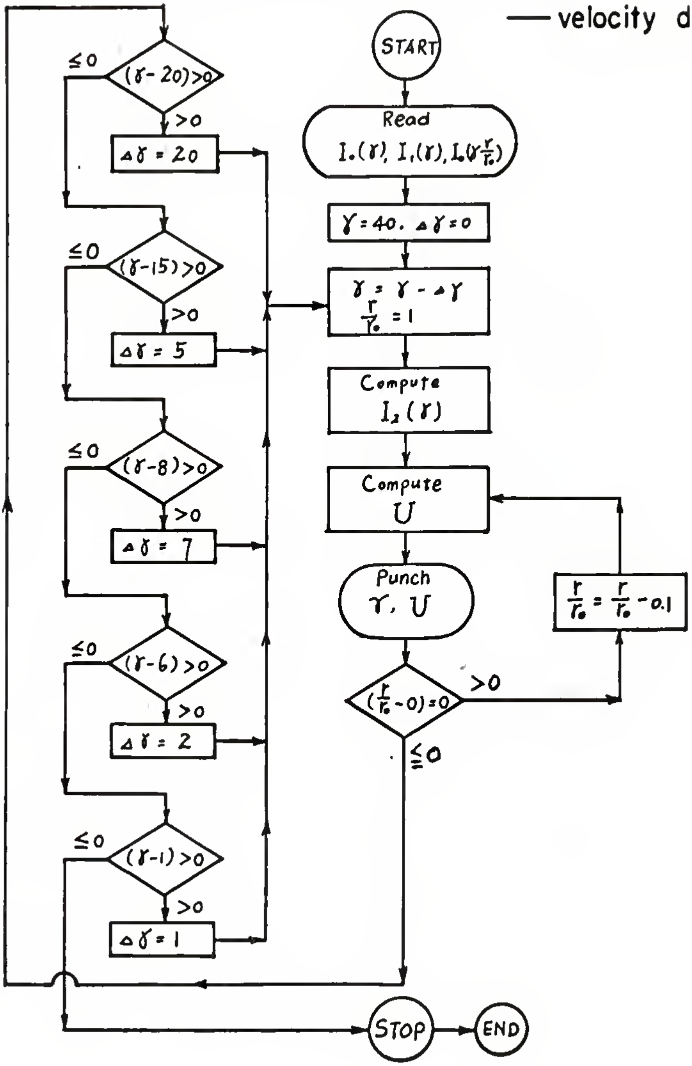

Table 3.8. Symbol Table

FORTRAN Symbol	Variables
BIO(N)	$I_0(\gamma)$
BI1(N)	$I_1(\gamma)$
BIOO(J)	$I_0(\frac{r}{r_0}\ \gamma)$
GAMA	γ
DELTG	$\Delta\ \gamma$
R	$\frac{r}{r_0}$
BI2N	$I_2(\gamma)$
U	$\frac{u}{\bar{u}}$

TABLE 3.9. FORTRAN PROGRAM FOR LANGHAAR'S METHOD
---VELOCITY DISTRIBUTION

```
C    C   LANGHAAR,S METHOD------VELOCITY DISTRIBUTION
    10 FORMAT(6E12.4)
    11 FORMAT(2I4,2F6.1,4E12.4)
    12 FORMAT(4X,I4,6X,F6.1,2E12.4)
       DIMENSION BIO(12),BI1(12),BIO0(120)
   100 READ 10, (BIO(N), N=1,10)
   101 READ 10, (BI1(N), N=1,10)
   102 READ 10, (BIO0(J), J=1,110)
       N=0
       J=0
       GAMA=40.
       DELTG=.0
     2 GAMA=GAMA-DELTG
       R=1.
       N=N+1
       J=J+1
       BI2N=-2.*BI1(N)/GAMA+BIO(N)
    20 U=(BIO(N)-BIO0(J))/BI2N
       IF(R-1.) 30,3,3
     3 PUNCH 11, N,J,GAMA,R,U,BIO0(J),BIO(N),BI1(N)
       GO TO 31
    30 PUNCH 12, J,R,U,BIO0(J)
       IF(R-0.) 32,32,31
    31 J=J+1
       R=R-.1
       GO TO 20
    32 IF(GAMA-20.) 41,41,4
     4 DELTG=20.
       GO TO 2
    41 IF(GAMA-15.) 5,5,42
    42 DELTG=5.
       GO TO 2
     5 IF(GAMA-8.) 6,6,51
    51 DELTG=7.
       GO TO 2
     6 IF(GAMA-6.) 7,7,61
    61 DELTG=2.
       GO TO 2
     7 IF(GAMA-1.) 8,8,71
    71 DELTG=1.
       GO TO 2
     8 STOP
       END
```

TABLF 3.10. NUMERICAL RFSULTS OF LANGHAAR'S METHOD
---VELOCITY DISTRIBUTION

N	J	GAMA	R	U	B100(J)	BIO(N)	BI1(N)
1	1	40.0	1.0	0.0000	0.1489E+17	0.1489E+17	0.1471E+17
	2		.9	0.1032E+01	0.2877E+15		
	3		.8	0.1052E+01	0.5591E+13		
	4		.7	0.1052E+01	0.1095E+12		
	5		.6	0.1052E+01	0.2169E+10		
	6		.5	0.1052E+01	0.4356E+08		
	7		.4	0.1052E+01	0.8934E+06		
	8		.3	0.1052E+01	0.1895E+05		
	9		.2	0.1052E+01	0.4276E+03		
	10		.1	0.1052E+01	0.1130E+02		
	11		0.0	0.1052E+01	0.1000E+01		
2	12	20.0	1.0	0.0000	0.4356E+08	0.4356E+08	0.4245E+08
	13		.9	0.9498	0.6218E+07		
	14		.8	0.1085E+01	0.8934E+06		
	15		.7	0.1105E+01	0.1294E+06		
	16		.6	0.1107E+01	0.1895E+05		
	17		.5	0.1108E+01	0.2816E+04		
	18		.4	0.1108E+01	0.4276E+03		
	19		.3	0.1108E+01	0.6723E+02		
	20		.2	0.1108E+01	0.1130E+02		
	21		.1	0.1108E+01	0.2280E+01		
	22		0.0	0.1108E+01	0.1000E+01		
3	23	15.0	1.0	0.0000	0.3396E+06	0.3396E+06	0.3281E+06
	24		.9	0.8776	0.7997E+05		
	25		.8	0.1084E+01	0.1895E+05		
	26		.7	0.1133E+01	0.4527E+04		
	27		.6	0.1144E+01	0.1094E+04		
	28		.5	0.1147E+01	0.2682E+03		
	29		.4	0.1148E+01	0.6723E+02		
	30		.3	0.1148E+01	0.1748E+02		
	31		.2	0.1148E+01	0.4881E+01		
	32		.1	0.1148E+01	0.1647E+01		
	33		0.0	0.1148E+01	0.1000E+01		
4	34	8.0	1.0	0.0000	0.4276E+03	0.4276E+03	0.3999E+03
	35		.9	0.6858	0.2029E+03		
	36		.8	0.1009E+01	0.9696E+02		
	37		.7	0.1162E+01	0.4674E+02		
	38		.6	0.1236E+01	0.2279E+02		

```
N   J  GAMA    R      U           BI00(J)      BI0(N)       BI1(N)

   39          .5  0.1271E+01  0.1130E+02
   40          .4  0.1288E+01  0.5747E+01
   41          .3  0.1296E+01  0.3049E+01
   42          .2  0.1300E+01  0.1750E+01
   43          .1  0.1302E+01  0.1167E+01
   44         0.0  0.1302E+01  0.1000E+01

5  45   6.0   1.0  0.0000      0.6723E+02  0.6723E+02  0.6134E+02
   46          .9  0.6032      0.3901E+02
   47          .8  0.9499      0.2279E+02
   48          .7  0.1150E+01  0.1344E+02
   49          .6  0.1265E+01  0.8028E+01

   50          .5  0.1333F+01  0.4881E+01
   51          .4  0.1372E+01  0.3049E+01
   52          .3  0.1395E+01  0.1990E+01
   53          .2  0.1407E+01  0.1394E+01
   54          .1  0.1414F+01  0.1092E+01
   55         0.0  0.1416E+01  0.1000E+01

6  56   5.0   1.0  0.0000      0.2724E+02  0.2724E+02  0.2434E+02
   57          .9  0.5576      0.1748E+02
   58          .8  0.9106      0.1130E+02
   59          .7  0.1135E+01  0.7378E+01
   60          .6  0.1277E+01  0.4881E+01

   61          .5  0.1368F+01  0.3290E+01
   62          .4  0.1426E+01  0.2280E+01
   63          .3  0.1462E+01  0.1647E+01
   64          .2  0.1484E+01  0.1266E+01
   65          .1  0.1495E+01  0.1063E+01
   66         0.0  0.1499E+01  0.1000E+01

7  67   4.0   1.0  0.0000      0.1130E+02  0.1130E+02  0.9759E+01
   68          .9  0.5096      0.8028E+01
   69          .8  0.8649      0.5747E+01
   70          .7  0.1113E+01  0.4157E+01
   71          .6  0.1285F+01  0.3049E+01

   72          .5  0.1405E+01  0.2280E+01
   73          .4  0.1487E+01  0.1750E+01
   74          .3  0.1543E+01  0.1394E+01
   75          .2  0.1578E+01  0.1167E+01
   76          .1  0.1598E+01  0.1040E+01
   77         0.0  0.1604E+01  0.1000E+01
```

```
 N    J   GAMA    R       U            BI00(J)       BI0(N)        BI1(N)

 8   78   3.0    1.0   0.0000        0.4881E+01    0.4881E+01    0.3953E+01
     79           .9   0.4627        0.3842E+01
     80           .8   0.8158        0.3049E+01
     81           .7   0.1084E+01    0.2446E+01
     82           .6   0.1287E+01    0.1990E+01

     83           .5   0.1440E+01    0.1647E+01
     84           .4   0.1553E+01    0.1394E+01
     85           .3   0.1633E+01    0.1213E+01
     86           .2   0.1687E+01    0.1092E+01
     87           .1   0.1718E+01    0.1023E+01
     88          0.0   0.1728E+01    0.1000E+01

 9   89   2.0    1.0   0.0000        0.2280E+01    0.2280E+01    0.1591E+01
     90           .9   0.4209        0.1990E+01
     91           .8   0.7692        0.1750E+01
     92           .7   0.1055E+01    0.1553E+01
     93           .6   0.1286E+01    0.1394E+01

     94           .5   0.1472E+01    0.1266E+01
     95           .4   0.1615E+01    0.1167E+01
     96           .3   0.1724E+01    0.1092E+01
     97           .2   0.1800E+01    0.1040E+01
     98           .1   0.1843E+01    0.1010E+01
     99          0.0   0.1858E+01    0.1000E+01

10  100   1.0    1.0   0.0000        0.1266E+01    0.1266E+01    0.5652
    101           .9   0.3909        0.1213E+01
    102           .8   0.7301        0.1167E+01
    103           .7   0.1032E+01    0.1126E+01
    104           .6   0.1283E+01    0.1092E+01

    105           .5   0.1497E+01    0.1063E+01
    106           .4   0.1667E+01    0.1040E+01
    107           .3   0.1792E+01    0.1023E+01
    108           .2   0.1888E+01    0.1010E+01
    109           .1   0.1940E+01    0.1003E+01
    110          0.0   0.1962E+01    0.1000E+01
```

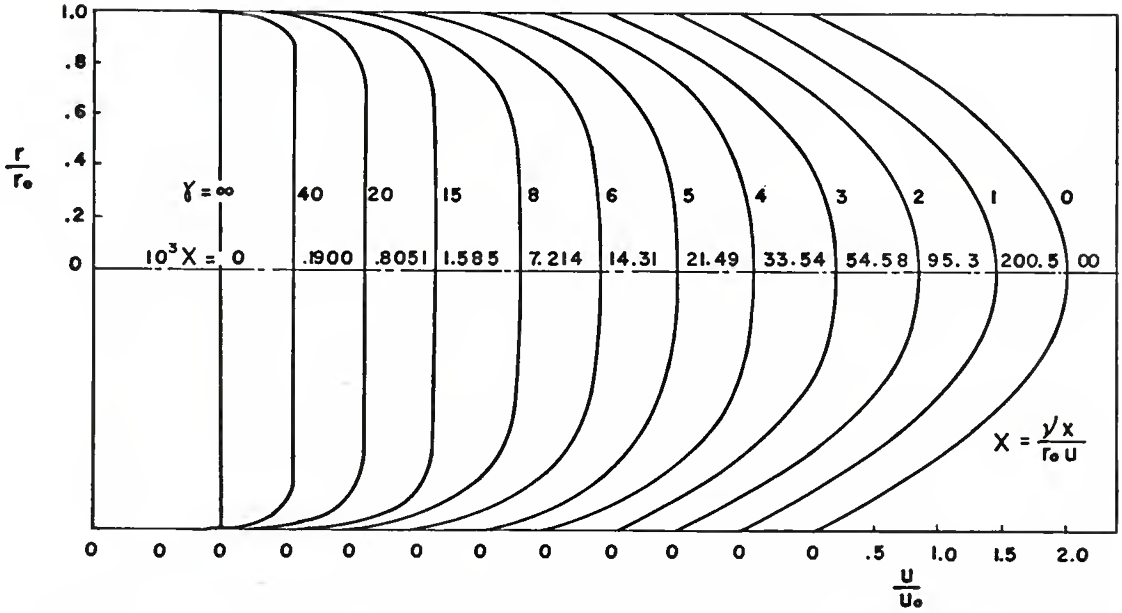

Fig. 3.2. Velocity distribution for laminar flow in the inlet section of a circular tube.

(3) Pressure Distribution

Equation (12) represents the total pressure drop between the supply reservoir and section x in the entrance region.

Let

$$\phi(\gamma) = \frac{\gamma^2}{I_2^2}\left[I_1^2 - I_0 I_2\right] \tag{16}$$

then we have

$$\int_0^X \frac{\gamma^2}{I_2^2}\left[I_1^2 - I_0 I_2\right] dX = \int_0^X \phi(\gamma)\,dX\ . \tag{17}$$

The evaluation of this integral is difficult due to the fact that $\phi(\gamma) \longrightarrow \infty$ as $x \longrightarrow 0$ $(\gamma \longrightarrow \infty)$. Therefore we make use of a limiting relation (see p. 100 in [2]) and obtain a result as follows:

$$X = \frac{1}{2}\int_\gamma^\infty (\gamma^{-3} + \ldots)d\gamma = \frac{1}{4\gamma^2} + \ldots\ .$$

It follows that

$$\lim_{\gamma \to \infty} \gamma^2 X = \frac{1}{4}\ .$$

It is pointed out by Langhaar that setting $\gamma^2 X = \frac{1}{4}$ in the range $\gamma \geqq 100$ is a good approximation. With this approximation the integration of equation (17) becomes easy and is carried out as follows:

$$\int_0^X \phi(\gamma)dX = \int_0^{.00002772} \phi(\gamma)dX + \int_{.00002772}^X \phi(\gamma)dX$$

where X = .00002772 corresponds to $\gamma = 100$. Furthermore, we can show (see [2], p. 104)

$$\frac{I_1^2}{I_2^2} - \frac{I_0}{I_2} \sim \frac{1}{\gamma} + \frac{3}{\gamma^2} + \frac{5}{\gamma^3} + \cdots .$$

Making the approximation that $\gamma^2 X = \frac{1}{4}$ for $\gamma \geq 100$, we obtain

$$\begin{aligned} \phi(\gamma) &= \gamma^2 \left(\frac{I_1^2}{I_2^2} - \frac{I_0}{I_2}\right) \\ &\sim \gamma + 3 + \frac{5}{8} \\ &\sim \frac{1}{2} X^{-\frac{1}{2}} + 3 + 10X^{\frac{1}{2}} \end{aligned}$$

and

$$\begin{aligned} \int_0^{.00002772} \phi(\gamma)dX &= \int_0^{.00002772} \left(\frac{1}{2} X^{-\frac{1}{2}} + 3 + 10X^{\frac{1}{2}}\right)dX \\ &= .00535 \end{aligned} \tag{18}$$

Therefore,

$$\int_0^X \phi(\gamma)dX = .00535 + \int_{.00002772}^X \phi(\gamma)dX$$

so that the numerical evaluation of equation (12), the pressure distribution, proceeds as follows:

(i) Evaluating $\int_0^X \emptyset(\gamma)dX$: The integral here represents the area under the curve in Fig. 3.3, part (b). The range of X is 0 to ∞, corresponding to the value of γ from ∞ to 0, and the range of $\emptyset(\gamma)$ is 0 to ∞, corresponding to the value of γ from 0 to ∞. Since the area under the curve corresponding to γ from ∞ to 100 has been evaluated as shown in equation (18), we will put $\gamma = 100$ as the initial value and assign a set of γ as indicated in Table 3.1. Then the X value for each γ can be computed by using equation (6) (also see Fig. 3.3, part (a)), and the value of $\emptyset(\gamma)$ can be computed from equation (16). The trapezoidal method is also applied in this numerical integration.

(ii) Evaluating $\int_0^1 (U^3-1)RdR$: For a given value of γ, this integral represents the area under the curve in Fig. 3.4. The range of R is 0 to 1. We will divide the range of R into 20 equi-distant intervals, so that the area is divided into 20 longitudinal strips and the total area is the sum of the areas of these strips. The area of each strip is evaluated by applying the trapezoidal method and the initial value is chosen at the origin. The value of $(U^3-1)R$ at a given value of γ can be computed by using equation (4) for different values of R.

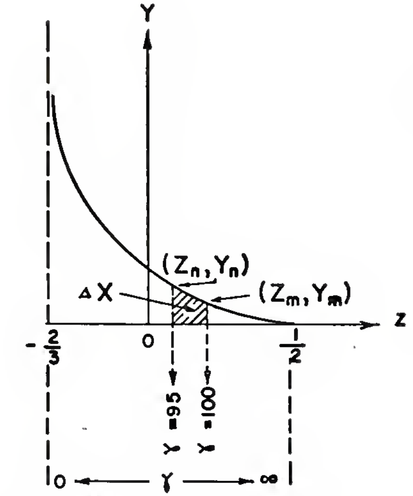

$$Z_m = 0.489$$

$$X_m = 0.00002772$$

$$\Delta Z = Z_n - Z_m$$

$$\Delta X = X_n - X_m$$

$$= \frac{Y_m + Y_n}{2} \cdot \Delta Z$$

$$X_n = X_m + \Delta X$$

Fig. 3.3-a. X_n represents the area under the curve in the interval.

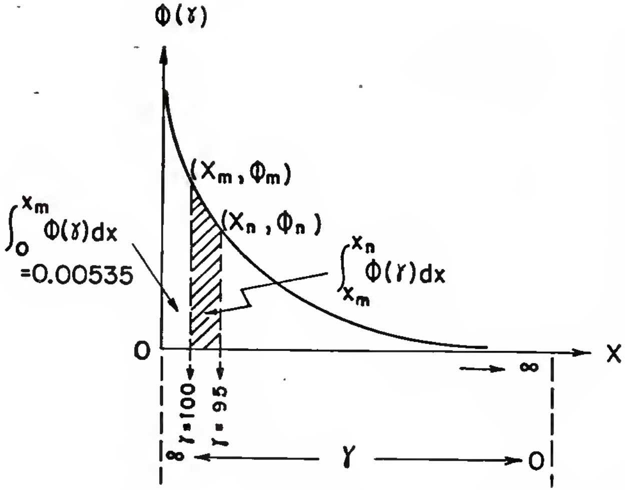

$$X_m = 0.00002772$$
$$\Phi_m = 110.534$$
$$\Delta X = X_n - X_m$$
$$\int_0^{X_m} \Phi(\gamma)dx = 0.00535$$
$$\int_{X_m}^{X_n} \Phi(\gamma)dx = \frac{\Phi_m + \Phi_n}{2} \cdot \Delta X$$
$$\int_0^{X_n} \Phi(\gamma)dx = \int_0^{X_m} \Phi(\gamma)dx + \int_{X_m}^{X_n} \Phi(\gamma)dx$$

Fig. 3.3-b. $\int_0^{X_n} \Phi(\gamma)dx$ represents the area under the curve in the interval $(0, X_n)$.

(iii) As soon as the above two integrals have been evaluated, the total pressure drop between the supply reservoir and section X in the entrance region corresponding to a certain value of γ can be computed from equation (12).

A flow chart (Table 3.10) will be followed by a symbol table (Table 3.11) and FORTRAN program (Table 3.12). The whole computation is carried out by using an IBM 1620 digital computer. It can be seen that in computing the pressure drop, the entrance length and the velocity distribution are computed at the same time. The statements from 430 to 47 in this program are inserted in order to punch out the different velocity values at different values of R when γ is equal to 8 and 7.5. The results are shown in Table 3.13 which can be compared with Table 3.5 and Table 3.10. The pressure distribution can be plotted from the results and is shown in Fig. 3.5.

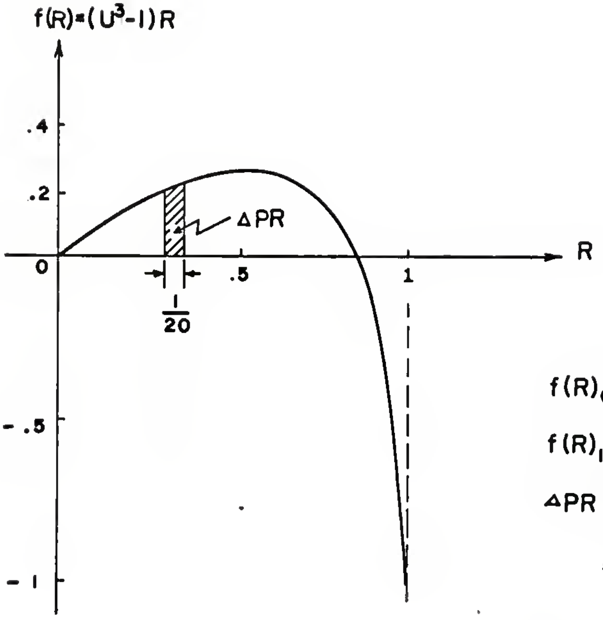

$$f(R)_0 = 0$$

$$f(R)_1 = (U^3-1)R_1$$

$$\Delta PR = \int_m^n (U^3-1)R\,dR = \frac{f(R)_m + f(R)_n}{2} \cdot \frac{1}{20}$$

$$PR = \int_0^1 (U^3-1)R\,dR = \sum_{\substack{m=0\\ n=1}}^{\substack{m=19\\ n=20}} \frac{f(R)_m + f(R)_n}{40}$$

Fig. 3.4. $\int_0^1 (U^3-1)R\,dR$ represents the area under the curve at a given value of Υ.

Table 3.10. Flow chart of Langharr's Method — pressure distribution

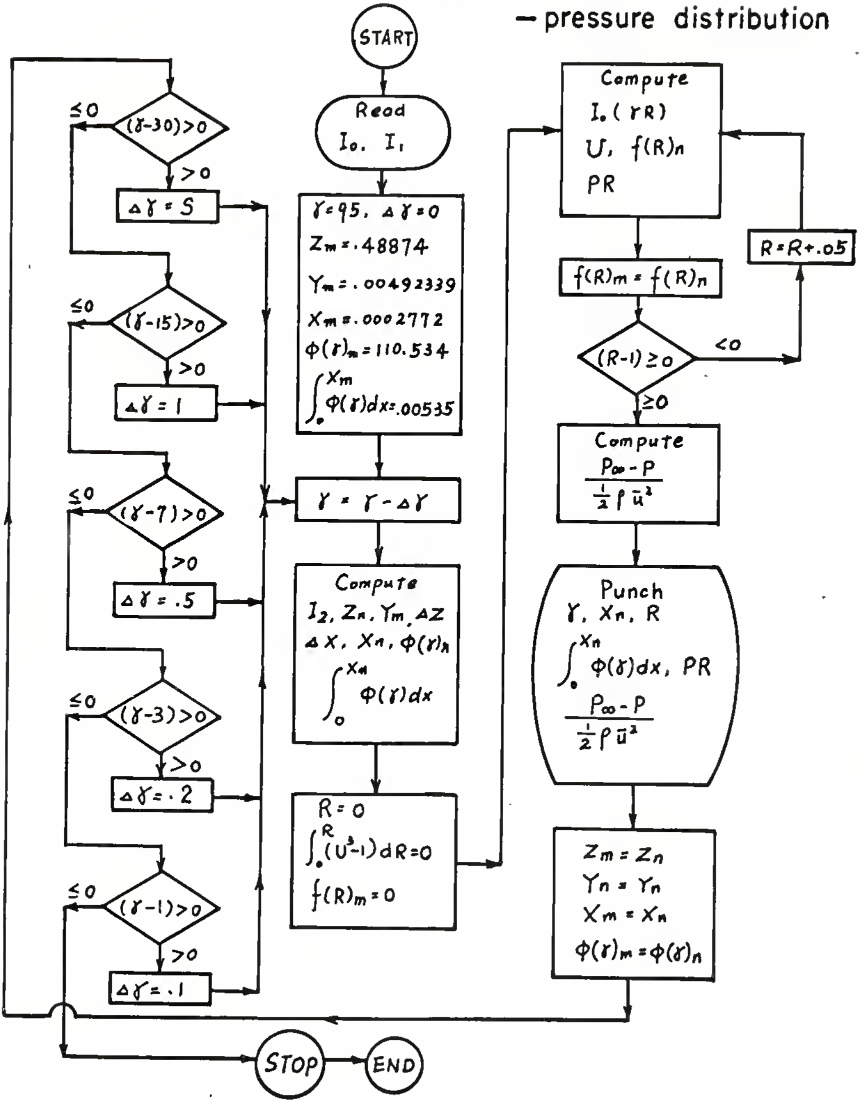

Table 3.11. Symbol Table

FORTRAN Symbol	Variable	FORTRAN Symbol	Variable
BIO(N)	$I_0(\gamma)$	FGN	$\phi(\gamma)_n$
BI1(N)	$I_1(\gamma)$	DPX	$\int_{X_m}^{X_n} \phi(\gamma)dX$
GAMA	γ	R	r/r_0
DELTG	$\Delta\ \gamma$	PR	$\int_0^1 (U^3-1)RdR$
ZM	Z_m	FRM	$(U^3-1)R_m$
YM	Y_m	H	$\gamma \cdot r/r_0$
XM	X_m	T	$(\gamma \frac{r}{r_0})/3.75$
FGM	$\phi(\gamma)_m$	E	$e = 2.71828$
PX	$\int_0^{X_m} \phi(\gamma)dX$	BIOH	$I_0(\gamma \cdot r/r_0)$
BI2N	$I_2(\gamma)$	U	$u/\bar{u}$
ZN	Z_n	FRN	$(U^3-1)R_n$
YN	Y_n	P	$(p_\infty - p)/\frac{1}{2}\rho\,\bar{u}^2$
DZ	$\Delta\ Z$		
DX	$\Delta\ X$		
XN	X_n		

TABLE 3. 12. FORTRAN PROGRAM FOR LANGHAAR'S METHOD
---PRESSURE DISTRIBUTION

```
C  C  LANGHAAR,S METHOD----PRESSURE DISTRIBUTION
  111 FORMAT(2E12.4)
    1 FORMAT(6E12.4)
   10 FORMAT(F5.1,E12.5,F7.3,E12.5)
   11 FORMAT(F5.1,E12.5,F7.3,12X,3E12.5)
   12 FORMAT(5X,12X,F7.3,E12.5,36X)
      DIMENSION BI0(100),BI1(100)
      READ 111,(BI0(N), N=1,2)
      READ 1,(BI0(N), N=3,94)
      READ 111, (BI1(N), N=1,2)
      READ 1, (BI1(N), N=3,94)
      N=0
      GAMA=95.
      DELTG=.0
      ZM=.488740
      YM=.00492339
      XM=.277177E-04
      FGM=110.534
      PX=.00535
    2 GAMA=GAMA-DELTG
      N=N+1
      BI2N=-2.*BI1(N)/GAMA+BI0(N)
      ZN=2.*BI0(N)/BI2N-((BI0(N)-1.)/BI2N)*((BI0(N)-1.)/BI2N)/2.
      ZN=ZN-(BI1(N)/BI2N)*(BI1(N)/BI2N)
      YN=BI2N/(2.*GAMA*BI1(N)-GAMA*GAMA)
      DZ=ZM-ZN
      DX=(YM+YN)*DZ/2.
      XN=DX+XM
    3 FGN=GAMA*GAMA*((BI1(N)/BI2N)*BI1(N)/BI2N -BI0(N)/BI2N)
      DPX=(FGN+FGM)*DX/2.
      PX=PX+DPX
   31 R=.0
      PR=.0
      FRM=.0
   40 R=R+.05
    4 H=GAMA*R
      T=H/3.75
      IF(H-3.75) 41,41,42
   41 BI0H=1.+3.5156229*T*T+3.0899424*T**4.+1.2067492*T**6.
      BI0H=BI0H+.2659732*T**8.+.0360768*T**10.+.0045813*T**12.
      GO TO 43
   42 E=2.71828
      BI0H=.398942+.0132859*T**(-1.)+.0022531*T**(-2.)-.0015756*T**(-3.)
      BI0H=BI0H+.00916281*T**(-4.)-.0205770*T**(-5.)+.0263554*T**(-6.)
      BI0H=(BI0H-.0164763*T**(-7.)+.0039237*T**(-8.))*E**H/H**(.5)
   43 U=(BI0(N)/BI2N)-BI0H/BI2N
  430 IF(GAMA-8.)44,44,431
```

```
 44 IF(GADA-7.5)431,45,45
 45 IF(R-.05)46,46,47
 46 PUNCH 10, GAMA,XN,R,U
    GO TO 431
 47 PUNCH 12, R,U
431 FRN=(U*U*U-1.)*R
    PR=PR+(FRN+FRM)*1./40.
    FRM=FRN
    IF(R-1.)40,471,471
471 P=1.+2.*(PX+PR)
    PUNCH 11, GAMA,XN,R,PX,PR,P
    ZM=ZN
    YM=YN
    XM=XN
    FGM=FGN
    IF(GAMA-30.)51,51,5
  5 DELTG=5.
    GO TO 2
 51 IF(GAMA-15.)61,61,6
  6 DELTG=1.
    GO TO 2
 61 IF(GAMA-7.)71,71,7
  7 DELTG=.5
    GO TO 2
 71 IF(GAMA-3.)81,81,8
  8 DELTG=.2
    GO TO 2
 81 IF(GAMA-.1)91,91,9
  9 DELTG=.1
    GO TO 2
 91 STOP
    END
```

TABLE 3. 13. NUMERICAL RESULTS OF LANGHAAR'S METHOD
---PRESSURE DISTRIBUTION

GAMA	XN	R	U	PX	PR	P
95.0	0.25698E-04	1.000		0.51415E-02	0.47856E-02	0.10199E+01
90.0	0.29600E-04	1.000		0.55078E-02	0.61964E-02	0.10234E+01
85.0	0.34632E-04	1.000		0.59607E-02	0.77159E-02	0.10274E+01
80.0	0.42129E-04	1.000		0.66132E-02	0.93582E-02	0.10319E+01
75.0	0.41607E-04	1.000		0.65713E-02	0.11102E-01	0.10353E+01
70.0	0.48340E-04	1.000		0.70578E-02	0.13005E-01	0.10401E+01
65.0	0.62291E-04	1.000		0.80185E-02	0.15084E-01	0.10462E+01
60.0	0.75165E-04	1.000		0.88649E-02	0.17343E-01	0.10524E+01
55.0	0.88917E-04	1.000		0.97001E-02	0.19824E-01	0.10590E+01
50.0	0.10613E-03	1.000		0.10648E-01	0.22591E-01	0.10665E+01
45.0	0.14100E-03	1.000		0.12406E-01	0.25776E-01	0.10764E+01
40.0	0.18997E-03	1.000		0.14699E-01	0.29533E-01	0.10885E+01
35.0	0.24726E-03	1.000		0.17111E-01	0.34100E-01	0.11024E+01
30.0	0.32532E-03	1.000		0.19935E-01	0.39973E-01	0.11198E+01
29.0	0.35222E-03	1.000		0.20812E-01	0.41385E-01	0.11244E+01
28.0	0.40884E-03	1.000		0.22640E-01	0.42975E-01	0.11312E+01
27.0	0.41100E-03	1.000		0.22707E-01	0.44512E-01	0.11344E+01
26.0	0.44713E-03	1.000		0.23777E-01	0.46259E-01	0.11401E+01
25.0	0.48918E-03	1.000		0.24981E-01	0.48145E-01	0.11463E+01
24.0	0.53170E-03	1.000		0.26155E-01	0.50175E-01	0.11527E+01
23.0	0.59418E-03	1.000		0.27821E-01	0.52411E-01	0.11605E+01
22.0	0.64747E-03	1.000		0.29190E-01	0.54810E-01	0.11680E+01
21.0	0.72095E-03	1.000		0.30999E-01	0.57465E-01	0.11769E+01
20.0	0.80507E-03	1.000		0.32988E-01	0.60403E-01	0.11868E+01
19.0	0.91111E-03	1.000		0.35395E-01	0.63682E-01	0.11982E+01
18.0	0.10386E-02	1.000		0.38177E-01	0.67306E-01	0.12110E+01
17.0	0.11916E-02	1.000		0.41377E-01	0.71396E-01	0.12255E+01
16.0	0.13659E-02	1.000		0.44855E-01	0.75962E-01	0.12416E+01
15.0	0.15845E-02	1.000		0.48999E-01	0.81156E-01	0.12603E+01
14.5	0.16941E-02	1.000		0.50986E-01	0.83984E-01	0.12699E+01
14.0	0.18650E-02	1.000		0.54002E-01	0.87132E-01	0.12823E+01
13.5	0.20142E-02	1.000		0.56569E-01	0.90420E-01	0.12940E+01
13.0	0.22174E-02	1.000		0.59962E-01	0.94031E-01	0.13080E+01
12.5	0.24347E-02	1.000		0.63492E-01	0.97932E-01	0.13228E+01
12.0	0.26687E-02	1.000		0.67176E-01	0.10208	0.13385E+01
11.5	0.29051E-02	1.000		0.70755E-01	0.10651	0.13545E+01
11.0	0.33235E-02	1.000		0.76910E-01	0.11170	0.13772E+01
10.5	0.37175E-02	1.000		0.82571E-01	0.11716	0.13995E+01
10.0	0.41649E-02	1.000		0.88776E-01	0.12313	0.14238E+01
9.5	0.47368E-02	1.000		0.96438E-01	0.12975	0.14524E+01
9.0	0.53627E-02	1.000		0.10452	0.13708	0.14832E+01
8.5	0.62083E-02	1.000		0.11504	0.14531	0.15207E+01

```
GAMA     XN          R          U                 PX               PR                 P

 8.0 0.72137E-02    .050 0.13020E+01
                    .100 0.13016E+01
                    .150 0.13009E+01
                    .200 0.12998E+01
                    .250 0.12982E+01

                    .300 0.12958E+01
                    .350 0.12925E+01
                    .400 0.12876E+01
                    .450 0.12806E+01
                    .500 0.12707E+01

                    .550 0.12563E+01
                    .600 0.12356E+01
                    .650 0.12057E+01
                    .700 0.11625E+01
                    .750 0.10999E+01

                    .800 0.10092E+01
                    .850 0.87742
                    .900 0.68578
                    .950 0.40678
                   1.000 0.12070E-03

 8.0 0.72137E-02   1.000                     0.12714          0.15453        0.15633E+01
 7.5 0.84253E-02    .050 0.13250E+01
                    .100 0.13244E+01
                    .150 0.13234E+01
                    .200 0.13219E+01
                    .250 0.13197E+01

                    .300 0.13166E+01
                    .350 0.13121E+01
                    .400 0.13059E+01
                    .450 0.12971E+01
                    .500 0.12849E+01

                    .550 0.12676E+01
                    .600 0.12434E+01
                    .650 0.12093E+01
                    .700 0.11611E+01
                    .750 0.10930E+01

                    .800 0.99666
                    .850 0.86014
                    .900 0.66646
                    .950 0.39136
                   1.000 0.20270E-03

 7.5 0.84253E-02   1.000                     0.14120          0.16481        0.16120E+01
 7.0 0.99027E-02   1.000                     0.15766          0.17627        0.16678E+01
 6.8 0.10786E-01   1.000                     0.16727          0.18180        0.16981E+01
 6.6 0.11531E-01   1.000                     0.17530          0.18702        0.17246E+01
 6.4 0.12334E-01   1.000                     0.18380          0.19258        0.17528E+01
```

```
GAMA      XN            R          U              PX            PR             P

 6.2 0.13271E-01   1.000                     0.19354       0.19851       0.17841E+01
 6.0 0.14313E-01   1.000                     0.20420       0.20474       0.18179E+01
 5.8 0.15465E-01   1.000                     0.21581       0.21139       0.18544E+01
 5.6 0.16716E-01   1.000                     0.22822       0.21832       0.18931E+01
 5.4 0.18092E-01   1.000                     0.24166       0.22558       0.19345E+01

 5.2 0.19668E-01   1.000                     0.25680       0.23333       0.19303E+01
 5.0 0.21487E-01   1.000                     0.27407       0.24183       0.20318E+01
 4.8 0.23337E-01   1.000                     0.29138       0.25019       0.20831E+01
 4.6 0.25455E-01   1.000                     0.31090       0.25926       0.21403E+01
 4.4 0.28020E-01   1.000                     0.33424       0.26939       0.22073E+01

 4.2 0.30859E-01   1.000                     0.35982       0.27983       0.22793E+01
 4.0 0.33536E-01   1.000                     0.38361       0.28972       0.23466E+01
 3.8 0.36722E-01   1.000                     0.41146       0.30061       0.24241E+01
 3.6 0.40524E-01   1.000                     0.44429       0.31236       0.25133E+01
 3.4 0.44671E-01   1.000                     0.47971       0.32430       0.26080E+01

 3.2 0.49436E-01   1.000                     0.51998       0.33678       0.27135E+01
 3.0 0.54582E-01   1.000                     0.56305       0.34942       0.28249E+01
 2.9 0.57869E-01   1.000                     0.59039       0.35659       0.28940E+01
 2.8 0.60976E-01   1.000                     0.61616       0.36304       0.29584E+01
 2.7 0.63876E-01   1.000                     0.64010       0.36939       0.30190E+01

 2.6 0.67533E-01   1.000                     0.67015       0.37603       0.30924E+01
 2.5 0.71746E-01   1.000                     0.70470       0.38359       0.31766E+01
 2.4 0.75624E-01   1.000                     0.73642       0.38994       0.32527E+01
 2.3 0.79693E-01   1.000                     0.76959       0.39696       0.33331E+01
 2.2 0.84457E-01   1.000                     0.80832       0.40344       0.34235E+01

 2.1 0.88231E-01   1.000                     0.83890       0.40895       0.34957E+01
 2.0 0.95300E-01   1.000                     0.89608       0.41794       0.36280E+01
 1.9 0.97764E-01   1.000                     0.91595       0.42204       0.36760E+01
 1.8 0.10291        1.000                     0.95724       0.42836       0.37712E+01
 1.7 0.10916        1.000                     0.10073E+01 0.43383       0.38823E+01

 1.6 0.12491        1.000                     0.11339E+01 0.44424       0.41563E+01
 1.5 0.12578        1.000                     0.11409E+01 0.44822       0.41783E+01
 1.4 0.14670        1.000                     0.13090E+01 0.45571       0.45295E+01
 1.3 0.15288        1.000                     0.13588E+01 0.46040       0.46385E+01
 1.2 0.14333        1.000                     0.12823E+01 0.46442       0.44935E+01

 1.1 0.18319        1.000                     0.16016E+01 0.47137       0.51459E+01
 1.0 0.20054        1.000                     0.17411E+01 0.47698       0.54361E+01
  .9 0.16526        1.000                     0.14584E+01 0.47732       0.48715E+01
  .8 0.18682E-01   1.000                     0.29524       0.48051       0.25315E+01
  .7 0.66941        1.000                     0.55116E+01 0.49384       0.13011E+02

  .6 0.24838        1.000                     0.21087E+01 0.48966       0.61968E+01
  .5 0.39536E+01   1.000                     0.32528E+02 0.50966       0.67074E+02
  .4 0.53580E+01   1.000                     0.44274E+02 0.49438       0.90536E+02
  .3-0.51193E+02   1.000                    -0.39828E+03 0.47521      -0.79461E+03
  .2 0.64759E+02   1.000                     0.49486E+03 0.49740       0.99171E+03
  .1-0.29826E+05   1.000                    -0.15259E+06 0.19272      -0.30517E+06
```

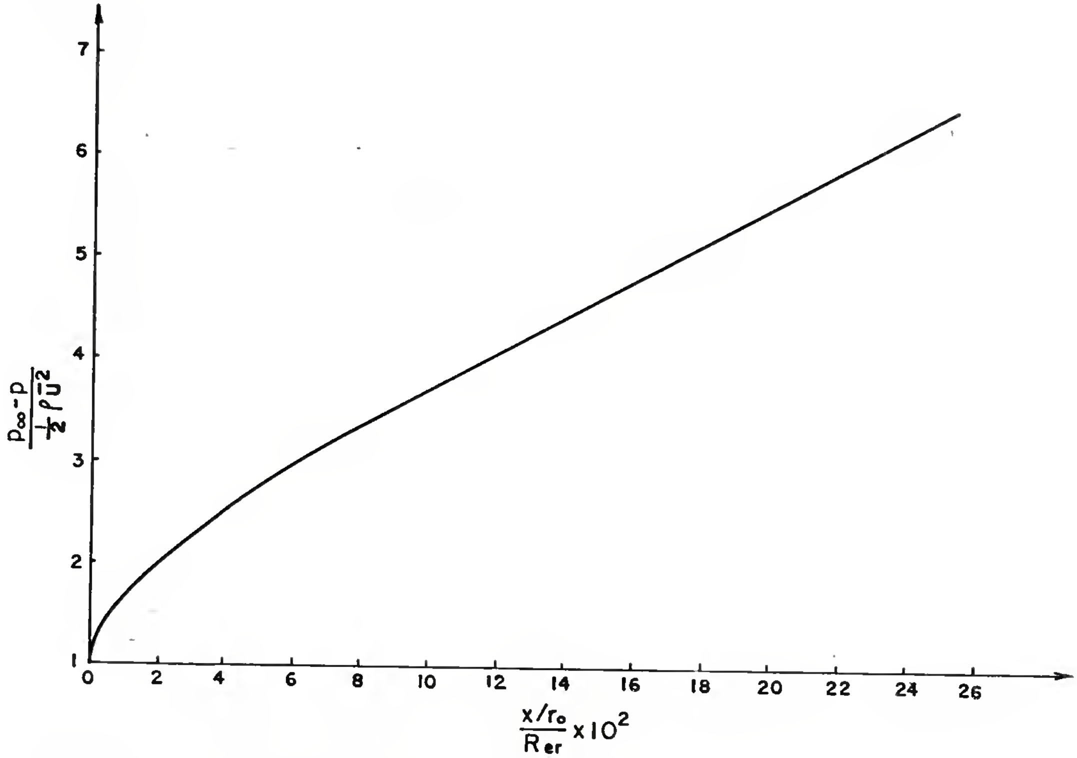

Fig. 3.5. Total pressure drops for laminar flow between the supply reservoir and the section X in the entrance region of a circular tube.

3.3. Results and Discussion

The results of the computed entrance length, velocity distribution and pressure drop in the entrance region by this method are shown with sample output data in Table 3.5, Table 3.10, and Table 3.13 and with plotted curves in Fig. 3.2 and Fig. 3.5.

Since the computational procedure is more complicated than that of Schiller's method, we separate it into three detailed FORTRAN programs. However, the whole computation may be put together into one FORTRAN program as described in section 3.2, part (iii). A more accurate pressure distribution may be obtained if we divide the range of R into 100 equi-distant intervals instead of 20. However, when we compare the results obtained in each case we find that at $\gamma = 20$, the error is only 1.8×10^{-4}, so that we can conclude that the division of range of R in 20 intervals provides sufficient precision for computing the pressure drops.

In the computational procedure the values of $I_0(\gamma)$ and $I_1(\gamma)$ are not computed. Although the equations representing $I_0(\gamma)$ and $I_1(\gamma)$ are available, the convergence of the series to obtain these values is too slow to compute these with the IBM 1620 computer. Therefore, the values of $I_0(\gamma)$ and $I_1(\gamma)$ are read in from an available reference [3].

The results of the present work are compared with those of Langhaar for some values of γ as shown in Table 3.14. Except for the results in the range of $\gamma < 1.2$, the results are nearly the same for $1.2 < \gamma < 100$. In the present work, for the region of $0 < \gamma < 1.2$, a reasonable result could not be obtained. The reason is unknown. In the near future, by using an IBM 360, much faster than an IBM 1620, we can compute $I_0(\gamma)$ and $I_1(\gamma)$ for the whole range concerned and we may be able to obtain more accurate results than formerly.

Table 3.14. Comparison of the present work with that from Langhaar

Y	Entrance Length X			Total Pressure Drop $\Delta p/\frac{1}{2}\ \bar{u}^{2}$			Center Line Velocity U_0		
	Present work	Langhaar's results	% differences	Present work	Langhaar's results	% differences	Present work	Langhaar's results	% differences
100	$.2772 \times 10^{-4}$	.000026	6.6	**	*	--	1.020	1.0203	.029
30	$.3253 \times 10^{-3}$	.000334	2.7	1.1198	*	--	1.070	1.0701	.0093
20	$.8051 \times 10^{-3}$	.000820	1.8	1.1868	1.2122	2.9	1.108	1.1079	.009
11	$.3324 \times 10^{-2}$	.00332	.09	1.3772	1.3866	.7	1.210	1.2095	.041
8	$.7214 \times 10^{-2}$	.00722	.01	1.5633	1.5732	.63	1.302	1.3021	.008
6	$.1431 \times 10^{-1}$	.0143	.07	1.8179	1.8300	.66	1.416	1.4157	.021
4	$.3354 \times 10^{-1}$	.0267	.09	2.3466	2.3614	.63	1.604	1.6041	.006
3	$.5458 \times 10^{-1}$	.0547	.54	2.8249	2.8474	.79	1.728	1.6961	.029
1.4	.1467	.1365	6.9	4.5295	4.3840	3.2	1.926	1.9245	.078

* : No available data listed in the original paper

** : No available data computed in the present work

REFERENCES

1. Langhaar, H. L., "Steady Flow in the Transition Length of a Straight Tube", Trans. of ASME, J. of Applied Mechanics, 64, A-55 (1942).

2. Li, K. C., "Analytical and Numerical Solutions of Some Entrance Region Flow Problems", M.S. Report, Mech. Engr., Kansas State University, Jan. 1966.

3. McClain, J. W., Schoenig, Jr., F. C. and Palladino, N. J., "Table of Bessel Functions to Argument 85", Engineering Research Bulletin B-85, The Pennsylvania State University, Sept. 1962.

4. McLachlan, N. W., "Bessel Functions for Engineers", Oxford University Press, 1934, p. 163.

5. Bennett, Milne, Bateman, "Numerical Integration of Differential Equations", Dover Publications, Inc., 1956, p. 30.

6. Abramowitz, Milton and Stegun, Irene A., "Handbook of Mathematical Functions with Formulas, Graphs, and Mathematical Tables", (AMS 55), June 1964, p. 378.

CHAPTER 4. SCHLICHTING'S MATCHING METHOD

4.1. Description of the Method [2, 10]

In this chapter we shall consider the case of flow in the inlet length of a straight channel with flat parallel walls. The flow field is assumed to be laminar, steady and two-dimensional and all fluid properties are considered to be constant. We also assume that the velocity in the inlet section is uniformly distributed over its width, 2a (Fig. 4.1). The governing boundary layer equation and continuity equation can be written as

$$u \frac{\partial u}{\partial x} + v \frac{\partial u}{\partial y} = - \frac{1}{\rho} \frac{dp}{dx} + \nu \frac{\partial^2 u}{\partial y^2} , \qquad (1)$$

$$\frac{\partial u}{\partial x} + \frac{\partial v}{\partial y} = 0 . \qquad (2)$$

A system of co-ordinates is used in which the axis of abscissas coincides with that of the channel (Fig. 4.1). For the expansion in the upstream direction we shall measure the ordinate y from the center-line of the channel, whereas for the expansion in the downstream direction the ordinate y' will be measured from one of the walls.

In this method the flow field is divided into two sections, the upstream and the downstream. In the upstream section, the boundary layers develop in a way similar to a flow over a flat plate with a pressure gradient in the direction of flow. The stream function and center line velocity are expanded in a power series, as in the case of the flat plate. The solution is found

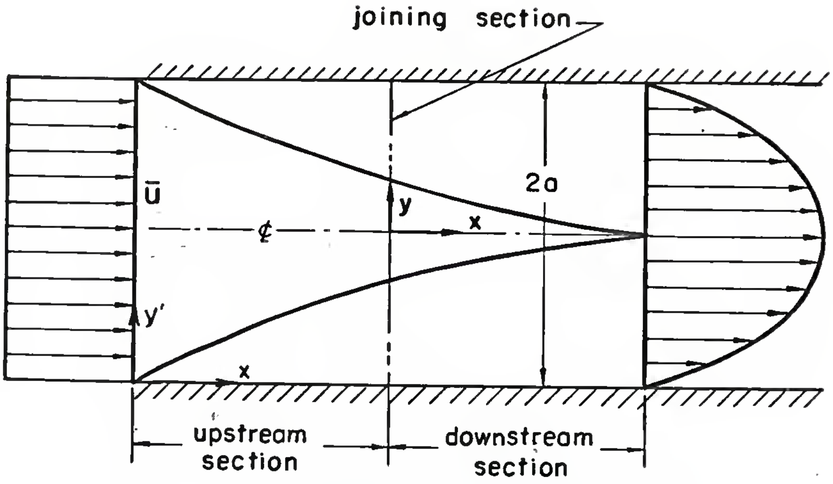

Fig.4.1. Configuration of a channel with parallel plates for matching method.

after the coefficients of the series are determined by substituting the assumed series into equation (1). For the downstream section, the velocity is assumed to be the sum of the fully developed parabolic velocity distribution and a deviation velocity which approaches zero as x ⟶ ∞. This deviation velocity is obtained by a series expansion in the upstream direction. Having obtained both solutions in the form of a series expansion, they are joined at a point where both solutions are valid. In this way an approximate description of the flow field in the entire region is obtained.

For the upstream solution, the center line velocity is assumed to be a series in ϵ.

$$u_0(x) = \bar{u}(1 + K_1\epsilon + K_2\epsilon^2 + \ldots) \tag{3}$$

where

$$\epsilon = \sqrt{\frac{\nu x}{a^2 \bar{u}}} ,$$

and K_1, K_2,... are constants to be determined.

Substituting the expression in equation (3) into the pressure gradient at the center line in the flow direction, we obtain

$$-\frac{1}{\rho}\frac{dp}{dx} = u_0\frac{du_0}{dx} = \frac{\bar{u}^2\epsilon}{2x}\Big[K_1 + (K_1^2 + 2K_2)\epsilon + 3(K_1K_2 + K_3)\epsilon^2 + \ldots\Big]. \tag{4}$$

It is also assumed that the stream function, $\psi(x,y')$, can be expanded into a series in ϵ

$$\psi(x,y') = \bar{u}a\left[\epsilon f_0(\eta) + \epsilon^2 f_1(\eta) + \dots\right] \tag{4a}$$

where

$$\eta = \sqrt{\frac{\bar{u}}{\nu x}} \cdot y' .$$

Then

$$u(x,y') = \frac{\partial\psi}{\partial y'} = \bar{u}\left[f_0'(\eta) + \epsilon f_1'(\eta) + \dots\right] . \tag{5}$$

$$\begin{aligned} v(x,y') = -\frac{\partial\psi}{\partial x} &= -\frac{\bar{u}a}{2x}\left[\epsilon f_0 + 2\epsilon^2 f_1 + 3\epsilon^2 f_2 + \dots\right] \\ &\quad + \frac{\bar{u}a\epsilon\eta}{2x}\left[f_0' + \epsilon f_1' + \epsilon^2 f_2' + \dots\right] . \end{aligned} \tag{6}$$

Substituting the expressions in equations (4), (5), and (6) into equation (1) and collecting terms in powers of ϵ, we obtain differential equations for f_0, f_1,... The equation of the first approximation (i.e. the zero power of ϵ) is

$$2f_0''' + f_0 f_0'' = 0 \tag{7}$$

with the boundary conditions

$$\left.\begin{aligned} f_0 = f_0' &= 0 \qquad \text{at} \qquad \eta = 0 , \\ f' &\longrightarrow 1 \qquad \text{at} \qquad \eta \longrightarrow \infty . \end{aligned}\right. \tag{7a}$$

This is identical with the differential equation of flow over a flat plate given and solved by Blasius. The second approximation (i.e. the first power of ϵ) is determined by the equation

$$2f_1''' + f_0 f_1'' - f_0' f_1' + 2f_0'' f_1 = -K_1 \tag{8}$$

which is a linear differential equation of third order. The boundary conditions are

$$f_1 = f_1' = 0 \qquad \text{at} \qquad \eta = 0 ,$$

$$f_1' = K_1 \qquad \text{at} \qquad \eta \longrightarrow \infty .$$

These differential equations can be solved numerically. With the values of f_0, f_1,... and K_1, K_2,... being found, the solution of the upstream section is complete.

For the downstream section, we assume

$$u(x,y) = u_f(y) - u^*(x,y) \tag{9}$$

where

$$u_f(y) = \frac{3}{2}\bar{u}(1 - \frac{y^2}{a^2})$$

is the fully developed parabolic velocity distribution and u* is the deviation velocity, which is assumed to be in the form

$$\frac{u^*}{\bar{u}} = c_1 e^{-\lambda_1 \epsilon^2} \psi_1'(\frac{y}{a}) . \tag{10}$$

Substituting the expressions in equations (9) and (10) into equation (1) yields the following differential equation for ψ_1:

$$\psi_1^{iv} + 3\lambda_1 \left[\frac{1}{2} (1 - \frac{y^2}{a^2}) \psi_1'' + \psi_1 \right] = 0 \tag{11}$$

with λ_1 as its eigenvalue. The boundary conditions are

$$\psi_1 = \psi_1'' = 0 \quad \text{at} \quad y = 0 ,$$

$$\psi_1 = \psi_1' = 0 \quad \text{at} \quad y = \pm a ,$$

$$\psi_1' = 1 \quad \text{at} \quad y = 0 .$$

The last boundary condition is chosen arbitrarily. This is possible since c_1 is still free. Having these boundary conditions, equation (11) can be solved by a power series method. Assume

$$\psi_1(\tfrac{y}{a}) = \sum_{n=0}^{\infty} A_n(\tfrac{y}{a})^n$$

$$= A_0 + A_1(\tfrac{y}{a}) + A_2(\tfrac{y}{a})^2 + \dots , \tag{12}$$

$$\psi_1'(\tfrac{y}{a}) = \sum_{n=1}^{\infty} n\, A_n(\tfrac{y}{a})^{n-1}$$

$$= A_1 + 2A_2(\tfrac{y}{a}) + 3A_3(\tfrac{y}{a})^2 + \dots , \tag{12a}$$

$$\psi_1''(\tfrac{y}{a}) = \sum_{n=2}^{\infty} n(n-1)A_n(\tfrac{y}{a})^{n-2}$$

$$= 2A_2 + 6A_3(\tfrac{y}{a}) + 12A_4(\tfrac{y}{a})^2 + \dots , \tag{12b}$$

$$\psi_1'''(\tfrac{y}{a}) = \sum_{n=3}^{\infty} n(n-1)(n-2)A_n(\tfrac{y}{a})^{n-3}$$

$$= 6A_3 + 24A_4(\tfrac{y}{a}) + 60A_5(\tfrac{y}{a})^2 + \dots , \tag{12c}$$

$$\psi_1^{iv}\left(\frac{y}{a}\right) = \sum_{n=4}^{\infty} n(n-1)(n-2)(n-3)A_n\left(\frac{y}{a}\right)^{n-4}$$

$$= 24A_4 + 120A_5\left(\frac{y}{a}\right) + 360A_6\left(\frac{y}{a}\right)^2 + \ldots \quad (12d)$$

By substituting the expressions in equations (12) to (12d) into equation (11), the recursion formula for A_n is obtained.

$$A_{n+4} = \frac{3\lambda_1 \ (n-2)(n+1)A_n - (n-1)(n+2)A_{n+2}}{2(n+1)(n+2)(n+3)(n+4)} .$$

The values of A_n and λ_1 can be obtained from this recursion formula together with the boundary conditions. Thus the deviation velocity is defined if c_1 is known, and c_1 can be determined in the process of matching both solutions.

The pressure drop in the upstream section is obtained from Euler's equation

$$-\frac{1}{\rho}\frac{dp}{dx} = u_0 \frac{du_0}{dx} . \quad (13)$$

The boundary layer thickness is very thin in this section and the flow is mostly irrotational in the central core. Integrating equation (13) gives the pressure drop between any two locations in the upstream section. On the other hand, the pressure drop in the downstream section involves the perturbation velocity, u*(x,y). Substituting the assumed velocity distribution in equation (9), into the boundary layer equation (1) and noting that the pressure varies with x only, we obtain

$$\frac{1}{\rho}\frac{dp}{dx} = \nu\left[-\frac{3\bar{u}}{a^2} - \frac{\bar{u}c_1}{a^2} e^{-\lambda_1\epsilon^2} \psi_1'''(1)\right] . \quad (14)$$

Integrating equation (14) from the joining section, ϵ^* to ϵ gives the pressure drop in the downstream section

$$\frac{p - p^*}{\frac{1}{2} \quad \bar{u}^2} = -6(\epsilon^2 - \epsilon^{*2}) + \frac{2c_1}{\lambda_1}\psi_1'''(1)(e^{-\lambda_1\epsilon^2} - e^{-\lambda_1\epsilon^{*2}}).$$

For the complete determination of the velocity distributions, as well as the pressure drops in the entire entrance region, only c_1 and ϵ^*, the location of the matching section, remain to be determined. This is done when the upstream and downstream solutions are matched. The conditions that the center line velocities of both isolations be equal and that the pressure gradient $\frac{dp}{dx}$ be identical at the matching section provide two simultaneous equations for c_1 and ϵ^* as follows:

$$1 + K_1\epsilon + K_2\epsilon^2 + K_3\epsilon^3 + K_4\epsilon^4 = \frac{3}{2} - c_1 e^{-\lambda_1\epsilon^2} . \qquad (15)$$

$$\frac{1}{2\epsilon}(1 + K_1\epsilon + K_2\epsilon^2 + K_3\epsilon^3 + K_4\epsilon^4)(K_1 + 2K_2\epsilon + 3K_3\epsilon^2 + 4K_4\epsilon^3)$$

$$= 3 + c_1 e^{-\lambda_1\epsilon^2} \psi_1'''(1) . \qquad (16)$$

Therefore c_1 and ϵ^* are determined from equations (15) and (16). The solution is then complete.

The detailed derivation of the equations is given in Li's report [1].

4.2. Computational Procedures

In this method the velocity distribution, pressure drops and entrance length in the whole entrance region can be represented numerically as soon as the following constants and functions are found. Those are:

(1) The functions $f_n(\eta)$ and their derivatives in equations (5) and (6).

(2) The constants K_n in equation (3).

(3) The eigenvalue λ_1 in equation (11).

(4) The constant c_1 and the value of ϵ in equations (15) and (16) at the matching point.

The values of $f_0(\eta)$ and its derivatives, K_1, λ_1, c_1 and ϵ have been obtained in the present work. We will proceed through the computational procedures in detail as follows:

(1) The Function $f_0(\eta)$ and its Derivatives

Equation (7),

$$f_0 f_0'' + 2f_0''' = 0 \tag{7}$$

with the boundary conditions given by equation (7a)

$$\left.\begin{array}{llll} f_0 = f_0' = 0 & \text{at} & \eta = 0 \\ f_0' \longrightarrow 1 & \text{as} & \longrightarrow \infty \end{array}\right\} \tag{7a}$$

has been solved by Blasius [5] using a series solution, by Töepfer [6] using the Runge-Kutta integration method, and by

Howarth [7] and others. Here, the solution is obtained by the Runge-Kutta integration method.

To integrate equation (7) numerically, another boundary value at $\eta = 0$ is required in order to start the integration. Thus we have to use a trial and error method assuming many different values to start the integration until we meet the third boundary condition $f_0' \longrightarrow 1$ as $\eta \longrightarrow \infty$. This difficulty can be avoided if we set

$$f_0(\eta) = AF(\xi) \qquad \text{where} \qquad \xi = B\eta$$

where A and B are arbitrary constants, then

$$\begin{aligned} f_0'(\eta) &= ABF'(\xi) , \\ f_0''(\eta) &= AB^2F''(\xi) , \\ f_0'''(\eta) &= AB^3F'''(\xi) . \end{aligned} \tag{17}$$

After substituting the above relations into equation (7), the transformed differential equation becomes

$$AB^3F''' + \frac{1}{2} A^2B^2FF'' = 0 \tag{18}$$

with the corresponding boundary conditions

$$\begin{aligned} F = F' = 0 \qquad &\text{at} \qquad \xi = 0 , \\ F' \longrightarrow \frac{1}{AB} \qquad &\text{as} \qquad \xi \longrightarrow \infty . \end{aligned} \tag{18a}$$

Equation (18) can be made identical with equation (7) if we set A = B. Then equation (17) becomes

$$2F''' + FF'' = 0 \tag{19}$$

with the boundary conditions

$$\begin{aligned} F = F' &= 0 \quad \text{at} \quad \xi = 0 \,, \\ F' &\rightarrow \frac{1}{A^2} \quad \text{as} \quad \xi \rightarrow \infty \,. \end{aligned} \tag{19a}$$

Now equation (19) can be integrated by giving an arbitrary third boundary value at $\xi = 0$. Solving $F(\xi)$ numerically, we can obtain the A value from the relation

$$A = \sqrt{\frac{1}{F'(\infty)}} \,.$$

Substituting the A value into equation (17), we finally get the right starting value from the relation

$$f_0''(0) = A^3 F''(0) \,. \tag{20}$$

Thus, in order to obtain the value of $f_0''(0)$ by integrating equation (19), we assume $F''(0) = 1$. This can be so assumed because A is an arbitrary value.

The Runge-Kutta method [4] is applied here to accomplish the numerical integration for equation (19). We will describe the key point of this method as follows

$$\frac{dF}{d\xi} = F' = f(\xi, F)$$

with initial values ξ_0 and F_0.

The increment for advancing the dependent variable is given by

$$\Delta F = \frac{1}{6}(K_1 + 2K_2 + 2K_3 + K_4)$$

where

$$K_1 = hf(\xi_0,\ F_0)$$

$$K_2 = hf(\xi_0 + \frac{1}{2}h,\quad F_0 + \frac{1}{2}K_1)$$

$$K_3 = hf(\xi_0 + \frac{1}{2}h,\quad F_0 + \frac{1}{2}K_2)$$

$$K_4 = hf(\xi_0 + h,\quad F_0 + K_3)$$

The values at $(\xi_1,\ F_1)$ are then given by

$$\xi_1 = \xi_0 + h, \qquad F_1 = F_0 + \Delta F\ .$$

The increment on F for the second intervals is computed by the same formulas, with $(\xi_0,\ F_0)$ replaced by $(\xi_1,\ F_1)$. Thus all intervals are computed in the same manner by using for the initial values those at the beginning of each interval. In order to facilitate the computation, let us employ a double subscript notation in which the first subscript denotes the interval in which we are working and the second the entries in the interval.

$$\xi_{11} = \xi_0, \quad F_{11} = F_0 \quad \text{and} \quad F'_{11} = f(\xi_0, F_0) = f(\xi_{11}, F_{11}).$$

Now we see that

$$K_1 = hf(\xi_0,\ F_0) = hF'_{11}$$

and

$$F_0 + \frac{1}{2}K_1 = F_0 + \frac{1}{2}hF'_{11} = F_0 + \frac{\Delta\xi}{2}F'_{11}\ .$$

Thus we have

$$\xi_{12} = \xi_{11} + \frac{\Delta\xi}{2}, \quad F_{12} = F_{11} + \frac{\Delta\xi}{2} F'_{11}, \quad F'_{12} = f(\xi_{12}, F_{12}).$$

Continuing, we see that

$$K_2 = hf(\xi_0 + \tfrac{1}{2} h, \; F_0 + \tfrac{1}{2} K_1) = \Delta\xi \, F'_{12}$$

$$K_3 = hf(\xi_0 + \tfrac{1}{2} h, \; F_0 + \tfrac{1}{2} K_2) = \Delta\xi \, F'_{13}$$

$$K_4 = hf(\xi_0 + h, \; F_0 + K_3) = \Delta\xi \, F'_{14}$$

so that

$$\Delta F_1 = \frac{\Delta\xi}{6} (F'_{11} + 2F'_{12} + 2F'_{13} + F'_{14})$$

The scheme of this method applied to solve equation (19) is shown partly in Table 4.1. Using this scheme it is easy to solve (19) and (7) because the equations are the same, only one of the boundary conditions (i.e. $F''(0)$ and $f''(0)$) is different. A flow chart (Table 4.2) is then constructed. First assume $F''(0) = 1$ and find the true value of $f''_0(0)$, then replace $F''(0)$ by $f''_0(0)$ and proceed with the same steps; the function $f_0(\eta)$ and its derivatives can be solved with no difficulty. The program for finding $f''_0(0)$ and for solving Blasius' differential equation is shown in Table 4.4. The numerical results for $f''_0(0)$ and $f_0(\eta)$ with its derivatives are shown in Table 4.5.

Table 4.1. Scheme of the Runge-Kutta Method in Solving Equation (19)

ξ	F	F'	F''	F'''
$\xi_{11} = \xi_0 = 0$	$F_{11} = F_0 = 0$	$F'_{11} = F'_0 = 0$	$F''_{11} = F''_0 = 1$	F'''_{11}
$\xi_{12} = \xi_{11} + \frac{\Delta\xi}{2}$	$F_{12} = F_{11} + F'_{11} \frac{\Delta\xi}{2}$	$F'_{12} = F'_{11} + F''_{11} \frac{\Delta\xi}{2}$	$F''_{12} = F''_{11} + F'''_{11} \frac{\Delta\xi}{2}$	F'''_{12}
$\xi_{13} = \xi_{11} + \frac{\Delta\xi}{2}$	$F_{13} = F_{11} + F'_{12} \frac{\Delta\xi}{2}$	$F'_{13} = F'_{11} + F''_{12} \frac{\Delta\xi}{2}$	$F''_{13} = F''_{11} + F'''_{12} \frac{\Delta\xi}{2}$	F'''_{13}
$\xi_{14} = \xi_{11} + \Delta\xi$	$F_{14} = F_{11} + F'_{13} \Delta\xi$	$F'_{14} = F'_{11} + F''_{13} \Delta\xi$	$F''_{14} = F''_{11} + F'''_{13} \Delta\xi$	F'''_{14}
		$\Delta F_1 = \frac{\Delta\xi}{6}(F'_{11} + 2F'_{12} + 2F'_{13} + F'_{14})$	$\Delta F'_1 = \frac{\Delta\xi}{6}(F''_{11} + 2F''_{12} + 2F''_{13} + F''_{14})$	$\Delta F'''$
$\xi_{21} = \xi_{11} + \Delta\xi$	$F_{21} = F_{11} + F_1$	$F'_{21} = F'_{11} + \Delta F'_1$	$F''_{21} = F''_{11} + \Delta F''_1$	F'''_{21}
$\xi_{22} = \xi_{21} + \frac{\Delta\xi}{2}$	$F_{22} = F_{21} + F_{21} \frac{\Delta\xi}{2}$	$F'_{22} = F'_{21} + F''_{21} \frac{\Delta\xi}{2}$	$F''_{22} = F''_{21} + F'''_{21} \frac{\Delta\xi}{2}$	F'''_{22}
------------	---------------	-------------------	-------------------	---

Table 4.2. Flow chart for finding $f_o(0)$ and solving Blasius differential equation.

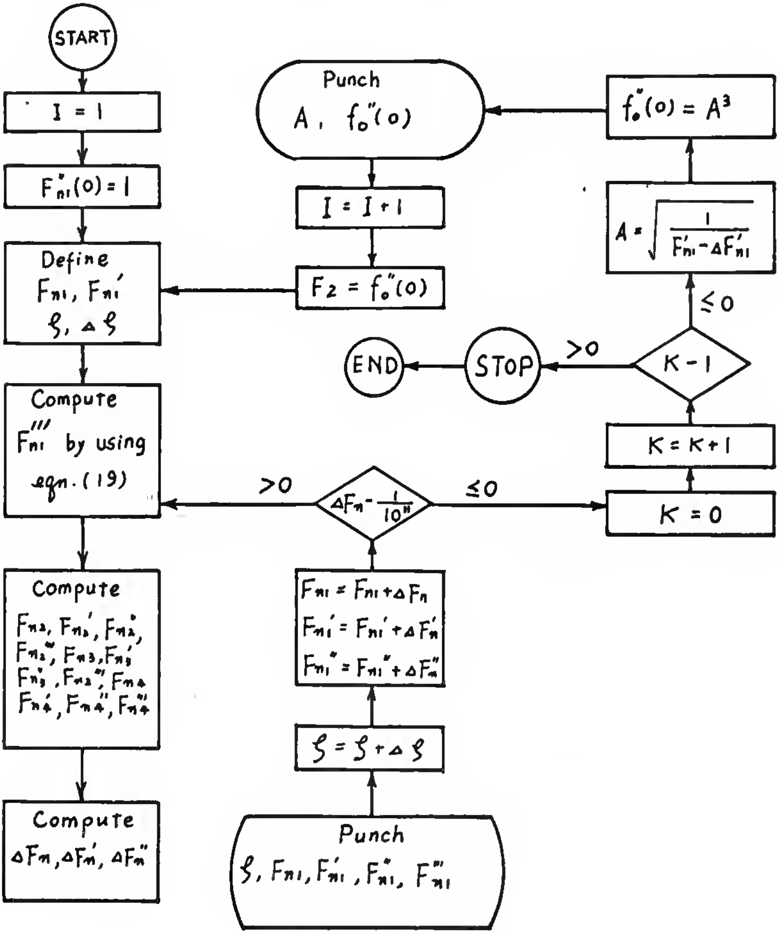
START
I = 1
$F''_{n1}(0) = 1$
Define F_{n1}, F'_{n1} $\xi, \Delta\xi$
Compute F'''_{n1} by using eqn. (19)
Compute $F_{n2}, F'_{n2}, F''_{n2}, F'''_{n2}, F_{n3}, F'_{n3}, F''_{n3}, F'''_{n3}, F_{n4}, F'_{n4}, F''_{n4}, F'''_{n4}$
Compute $\Delta F_n, \Delta F'_n, \Delta F''_n$
Punch A, $f''_o(0)$
I = I + 1
$F_2 = f''_o(0)$
$f''_o(0) = A^3$
$A = \sqrt{\frac{1}{F'_{n1} - \Delta F'_{n1}}}$
≤0
>0
K − 1
STOP
END
K = K + 1
K = 0
$\Delta F_n - \frac{1}{10^n}$
>0
≤0
$F_{n1} = F_{n1} + \Delta F_n$
$F'_{n1} = F'_{n1} + \Delta F'_n$
$F''_{n1} = F''_{n1} + \Delta F''_n$
$\xi = \xi + \Delta\xi$
Punch $\xi, F_{n1}, F'_{n1}, F''_{n1}, F'''_{n1}$

Table 4.3. Symbol Table

Variable	FORTRAN Symbol	Variable	FORTRAN Symbol
ξ	E	F_{n4}	FC
$\Delta\xi$	DE	F'_{n4}	F1C
F_{n1}	F	F''_{n4}	F2C
F'_{n1}	F1	F'''_{n4}	F3C
F''_{n1}	F2	ΔF_n	DF
F'''_{n1}	F3	$\Delta F'_1$	DF1
F_{n2}	FA	$\Delta F''_1$	DF2
F'_{n2}	F1A	A	A
F''_{n2}	F2A	$f''_0(0)$	F20
F'''_{n2}	F3A		
F_{n3}	FB		
F'_{n3}	F1B		
F''_{n3}	F2B		
F'''_{n3}	F3B		

Note: When I=2 in the Table 4.2, all functions F are changed into functions f_0 and ξ is changed into η.

TABLE 4.4. FORTRAN PROGRAM FOR FINDING $f_0''(0)$ AND SOLVING BLASIUS DIFFERENTIAL EQUATION

```
C   C   MATCHING METHOD---FINDING  F20  AND SOLVING BLASIUS DIFF. EQU.
  101 FORMAT(5E14.6)
  102 FORMAT(/3H A=E14.6)
  103 FORMAT(/5H F20=E12.6)
      I=1
      F2=1.0
    1 E=.0
      DE=.01
      F=.0
      F1=.0
    2 F3=-F*F2/2.
      FA=F+F1*DE/2.
      F1A=F1+F2*DE/2.
      F2A=F2+F3*DE/2.
      F3A=-FA*F2A/2.
    3 FB=F+F1A*DE/2.
      F1B=F1+F2A*DE/2.
      F2B=F2+F3A*DE/2.
      F3B=-FB*F2B/2.
    4 FC=F+F1B*DE
      F1C=F1+F2B*DE
      F2C=F2+F3B*DE
      F3C=-FC*F2C/2.
    5 DF=(F1+2.*F1A+2.*F1B+F1C)*DE/6.
      DF1=(F2+2.*F2A+2.*F2B+F2C)*DE/6.
      DF2=(F3+2.*F3A+2.*F3B+F3C)*DE/6.
      PUNCH 101, E,F,F1,F2,F3
    6 E=E+DE
      F=F+DF
      F1=F1+DF1
      F2=F2+DF2
   61 IF(DF1-.100000E-10)8,8,2
    8 K=0
      K=K+1
      IF(K-1)9,9,10
    9 A=SQRTF(1./(F1-DF1))
      PUNCH 102, A
      F20=A*A*A
      PUNCH 103, F20
      I=I+1
      F2=F20
      GO TO 1
   10 STOP
      END
```

TABLE 4.5. NUMERICAL RESULTS OF $f_0''(\eta)$ AND SOLUTION OF BLASIUS DIFFERENTIAL EQUATION

```
A=   0.692479

F20=0.332063

      E               F              F1             F2              F3

   .000000       0.000000       0.000000       0.332063        0.000000
   .100000       0.166031E-02   0.332061E-01   0.332054       -0.275656E-03
   .200000       0.664111E-02   0.664089E-01   0.331990       -0.110239E-02
   .300000       0.149417E-01   0.996003E-01   0.331815       -0.247894E-02
   .400000       0.265603E-01   0.132766       0.331476       -0.440205E-02

   .500000       0.414935E-01   0.165888       0.330917       -0.686545E-02
   .600000       0.597356E-01   0.198941       0.330085       -0.985892E-02
   .700000       0.812783E-01   0.231894       0.328928       -0.133674E-01
   .800000       0.106110       0.264714       0.327395       -0.173699E-01
   .900000       0.134215       0.297359       0.325439       -0.218394E-01

   .100000E+01   0.165574       0.329786       0.323013       -0.267413E-01
   .110000E+01   0.200163       0.361944       0.320077       -0.320339E-01
   .120000E+01   0.237952       0.393783       0.316595       -0.376673E-01
   .130000E+01   0.278907       0.425244       0.312534       -0.435841E-01
   .140000E+01   0.322987       0.456269       0.307871       -0.497191E-01

   .150000E+01   0.370144       0.486797       0.302586       -0.560002E-01
   .160000E+01   0.420327       0.516765       0.296669       -0.623490E-01
   .170000E+01   0.473477       0.546110       0.290117       -0.686817E-01
   .180000E+01   0.529526       0.574768       0.282936       -0.749110E-01
   .190000E+01   0.588405       0.602676       0.275141       -0.809472E-01

   .200000E+01   0.650035       0.629776       0.266756       -0.867003E-01
   .210000E+01   0.714331       0.656009       0.257813       -0.920821E-01
   .220000E+01   0.781206       0.681321       0.248355       -0.970081E-01
   .230000E+01   0.850563       0.705664       0.23843        -0.101400
   .240000E+01   0.922305       0.728994       0.228095       -0.105187

   .250000E+01   0.996327       0.751272       0.217415       -0.108308
   .260000E+01   0.107252E+01   0.772467       0.206458       -0.110715
   .270000E+01   0.115076E+01   0.792556       0.195297       -0.112372
   .280000E+01   0.123100E+01   0.811522       0.184009       -0.113257
   .290000E+01   0.131305E+01   0.829356       0.172671       -0.113363

   .300000E+01   0.139683E+01   0.846057       0.161362       -0.112698
   .310000E+01   0.148222E+01   0.861632       0.150157       -0.111283
   .320000E+01   0.156912E+01   0.876095       0.139129       -0.109155
   .330000E+01   0.165740E+01   0.889466       0.128348       -0.106362
   .340000E+01   0.174697E+01   0.901775       0.117877       -0.102964
```

```
       E               F            F1              F2             F3

 0.350000E+01   0.183772Γ+01   0.913054       0.107773       -0.990289E-01
 0.360000E+01   0.192955L+01   0.923^43       0.980870E-01   -0.946319E-01
 0.370000E+01   0.202236E+01   0.932u86       0.888599E-01   -0.898533E-01
 0.380000E+01   0.211606E+01   0.941131       0.801263E-01   -0.847759E-01
 0.390000E+01   0.221056E+01   0.948729       0.719119E-01   -0.794827E-01

 0.400000E+01   0.230577E+01   0.955532       0.642342E-01   -0.740549E-01
 0.410000E+01   0.240164E+01   0.961594       0.571028E-01   -0.685701E-01
 0.420000E+01   0.249807E+01   0.966970       0.505197E-01   -0.631009E-01
 0.430000E+01   0.259501E+01   0.971716       0.444800E-01   -0.577129E-01
 0.440000E+01   0.269239E+01   0.975884       0.389725E-01   -0.524646E-01

 0.450000E+01   0.279017E+01   0.979527       0.339807E-01   -0.474059E-01
 0.460000E+01   0.288828E+01   0.982696       0.294836E-01   -0.425784E-01
 0.470000E+01   0.298669E+01   0.985440       0.254562E-01   -0.380149E-01
 0.480000E+01   0.308536E+01   0.987802       0.218710E-01   -0.337399E-01
 0.490000E+01   0.318424E+01   0.989827       0.186981E-01   -0.297696E-01

 0.500000E+01   0.328331E+01   0.991555       0.159066E-01   -0.261132E-01
 0.510000E+01   0.338254E+01   0.993020       0.134649E-01   -0.227728E-01
 0.520000E+01   0.348191E+01   0.994258       0.113416E-01   -0.197452E-01
 0.530000E+01   0.358138E+01   0.995298       0.950575E-02   -0.170219E-01
 0.540000E+01   0.368096E+01   0.996168       0.792751E-02   -0.145904E-01

 0.550000E+01   0.378061E+01   0.996891       0.657845E-02   -0.124353E-01
 0.560000E+01   0.388033E+01   0.997490       0.543183E-02   -0.105387E-01
 0.570000E+01   0.398011E+01   0.997983       0.446275E-02   -0.888112E-02
 0.580000E+01   0.407992E+01   0.998388       0.364831E-02   -0.744242E-02
 0.590000E+01   0.417978E+01   0.998717       0.296766E-02   -0.620208E-02

 0.600000E+01   0.427967E+01   0.998985       0.240197E-02   -0.513980E-02
 0.610000E+01   0.437957E+01   0.999201       0.193442E-02   -0.423596E-02
 0.620000E+01   0.447950E+01   0.999374       0.155012E-02   -0.347188E-02
 0.630000E+01   0.457945E+01   0.999513       0.123597E-02   -0.283003E-02
 0.640000E+01   0.467940E+01   0.999623       0.980577E-03   -0.229426E-02

 0.650000E+01   0.477937E+01   0.999711       0.774077E-03   -0.184980E-02
 0.660000E+01   0.487934E+01   0.999780       0.608018E-03   -0.148336E-02
 0.670000E+01   0.497932E+01   0.999833       0.475201E-03   -0.118309E-02
 0.680000E+01   0.507931Γ+01   0.999875       0.369545E-03   -0.938516E-03
 0.690000E+01   0.517930L+01   0.999^08       0.285947E-03   -0.740503E-03

 0.700000E+01   0.527929E+01   0.999933       0.220157E-03   -0.581137E-03
 0.710000E+01   0.537928E+01   0.999952       0.168659E-03   -0.453632E-03
 0.720000E+01   0.547928E+01   0.999967       0.128562E-03   -0.352215E-03
 0.730000E+01   0.557928E+01   0.999978       0.975096E-04   -0.272016E-03
 0.740000E+01   0.567927E+01   0.999987       0.735884E-04   -0.208964E-03
```

```
      E              F             E1             F2            E3

0.750000E+01  0.577927E+01  0.999993      0.552586E-04 -0.159677E-03
0.760000E+01  0.587927E+01  0.999998      0.412875E-04 -0.121370E-03
0.770000E+01  0.597927E+01  0.100000E+01  0.306949E-04 -0.917666E-04
0.780000E+01  0.607927E+01  0.100000E+01  0.227061E-04 -0.690182E-04
0.790000E+01  0.617927E+01  0.100000E+01  0.167127E-04 -0.516362E-04

0.800000E+01  0.627927E+01  0.100001E+01  0.122400E-04 -0.384290E-04
0.810000E+01  0.637927E+01  0.100001E+01  0.891954E-05 -0.284501E-04
0.820000E+01  0.647927E+01  0.100001E+01  0.646744E-05 -0.209521E-04
0.830000E+01  0.657927E+01  0.100001E+01  0.466607E-05 -0.153497E-04
0.840000E+01  0.667927E+01  0.100001E+01  0.334964E-05 -0.111866E-04

0.850000E+01  0.677927E+01  0.100001E+01  0.239262E-05 -0.811012E-05
0.860000E+01  0.687927E+01  0.100001E+01  0.170051E-05 -0.584913E-05
0.870000E+01  0.697927E+01  0.100001E+01  0.120257E-05 -0.419654E-05
0.880000E+01  0.707927E+01  0.100001E+01  0.846200E-06 -0.299524E-05
0.890000E+01  0.717927E+01  0.100001E+01  0.592465E-06 -0.212673E-05

0.900000E+01  0.727927E+01  0.100001E+01  0.412745E-06 -0.150224E-05
0.910000E+01  0.737927E+01  0.100001E+01  0.286107E-06 -0.105563E-05
0.920000E+01  0.747927E+01  0.100001E+01  0.197335E-06 -0.737961E-06
0.930000E+01  0.757927E+01  0.100001E+01  0.135428E-06 -0.513222E-06
0.940000E+01  0.767927E+01  0.100001E+01  0.924785E-07 -0.355084E-06

0.950000E+01  0.777927E+01  0.100001E+01  0.628350E-07 -0.244405E-06
0.960000E+01  0.787927E+01  0.100001E+01  0.424807E-07 -0.167358E-06
0.970000E+01  0.797927E+01  0.100001E+01  0.285765E-07 -0.114010E-06
0.980000E+01  0.807927E+01  0.100001E+01  0.191274E-07 -0.772678E-07
0.990000E+01  0.817927E+01  0.100001E+01  0.127389E-07 -0.520974E-07

0.100000E+02  0.827927E+01  0.100001E+01  0.844180E-08 -0.349460E-07
0.101000E+02  0.837927E+01  0.100001E+01  0.556631E-08 -0.233208E-07
0.102000E+02  0.847927E+01  0.100001E+01  0.365198E-08 -0.154831E-07
0.103000E+02  0.857927E+01  0.100001E+01  0.238406E-08 -0.102268E-07
0.104000E+02  0.867927E+01  0.100001E+01  0.154859E-08 -0.672030E-08
0.105000E+02  0.877927E+01  0.100001E+01  0.100088E-08 -0.439350E-08
```

(2) K_1 Value

By substituting the expressions in equations (4), (5), and (6) into equation (1) and colleoting terms in powers of ϵ, we obtain differential equations (7) and (8)

$$2f_0''' + f_0 f_0'' = 0 \tag{7}$$

$$2f_1''' + f_0 f_1'' - f_0' f_1' + 2f_0'' f_1 = -K_1 \; . \tag{8}$$

We can go further by collecting ϵ^3 terms and obtain another differential equation such as

$$(f_1')^2 + 2f_0' f_2' - f_0 f_2'' - 2f_1 f_1'' - 3f_2 f_0'' - 2f_2''' = K_1^2 + 2K_2 \tag{21}$$

and so on.

The boundary conditions for these equations are determined from u=0 and v=0 at the wall (see equations (5) and (6)), and become

$$f_0(0) = f_1(0) = f_2(0) = \dots = f_n(0) = 0$$

$$f_0'(0) = f_1'(0) = f_2'(0) = \dots = f_n'(0) = 0 \; .$$

At the edge of the boundary layer, $\eta \sim \infty$ and $u = u_0(x)$ so that equating equations (3) and (5) and collecting coefficients of like powers of ϵ yields

$$
\begin{aligned}
f_0'(\infty) &= 1 \\
f_1'(\infty) &= K_1 \\
&\vdots \\
f_n'(\infty) &= K_n\ .
\end{aligned}
$$

For large η, the foregoing relations may be integrated to yield the approximate relations

$$
\begin{aligned}
f_0 &\sim \eta + A_0 \\
f_1 &\sim K_1\eta + A_1 \\
f_2 &\sim K_2\eta + A_2 \\
&\vdots \\
f_n &\sim K_n\eta + A_n\ .
\end{aligned}
\tag{22}
$$

Further, from the continuity equation one obtains

$$\bar{u}a = \int_0^u udy = \left[\psi(x,y')\right]_{y'=a}\ .$$

At the center line of the duct η is large and equations (22) are valid. In addition, at y=a we find that $\eta = 1/\epsilon$. Using these relations in the foregoing equation together with equation (4a), we obtain

$$\psi(x,y') = \bar{u}a\left[\epsilon(\tfrac{1}{\epsilon} + A_0) + \epsilon^2(\tfrac{K_1}{\epsilon} + A_1) + \epsilon^3(\tfrac{K_2}{\epsilon} + A_2) + \ldots\right]$$

$$1 = \left[(1 + \epsilon A_0) + (K_1\epsilon + \epsilon^2 A_1) + (K_2\epsilon^2 + \epsilon^3 A_2) + \ldots\right]$$

or $K_1 = -A_0$, $K_2 = -A_1$, $K_3 = -A_2 \ldots K_n = -A_{n-1}$. Therefore, when equations (7), (8), (21) and so on are integrated numerically, the function f_n will asymptotically approach the expression

$$f_n = K_n \cdot \eta - K_{n+1} \tag{23}$$

for large values of η. In this manner, the K_n-values needed in each equation can be determined from the solution of the preceding equation of the set (7), (8), (21) and so on.

Now let n=0, then from equation (3) $K_0 = 1$, and using the last output data in Table 4.5, one obtains

$$K_1 = 10.5 - 0.877927 = 1.72073 .$$

$K_1 = 1.72$ was computed by Schlichting [2].

(3) The Eigenvalue λ_1

The function $\psi_1(\frac{y}{a})$ is assumed in series form as shown in equation (12). The coefficient A_n can be expressed by a recursion formula as

$$A_{n+4} = \frac{3\lambda_1\left[(n-2)(n+1)A_n - (n-1)(n+2)A_{n+2}\right]}{2(n+1)(n+2)(n+3)(n+4)} \quad \text{when} \quad n \geq 0 \tag{24}$$

or

$$A_n = \frac{3}{2}\lambda_1\left[\frac{(n-6)(n-3)A_{n-4} - (n-2)(n-3)A_{n-2}}{n(n-1)(n-2)(n-3)}\right] \quad \text{when} \quad n \geq 4. \tag{24a}$$

From the boundary condition $\psi_1(0) = 0$, we find from equations (12) and (24) that A_0 and all constants with even subscripts are zero. From $\psi_1'(0) = 1$ and equation (12b), A_1 is found to be one. This leaves two boundary conditions, $\psi_1(\pm 1) = \psi_1'(\pm 1) = 0$, to determine the eigenvalue λ_1 and A_3. Since these boundary conditions are in the form of an infinite series, there is no simple method of calculating λ_1 and A_3. A trial and error method is then used. If a value of λ_1 is chosen, then values of A_n can be found in terms of A_3. Fifty terms are used by test in calculating the summation of the series to assume a small error. Using the boundary condition $\psi_1(\pm 1) = 0$, A_3 is found. These values of A_3 and λ_1 are then checked with the last remaining boundary condition $\psi_1'(\pm 1) = 0$. If these values do not satisfy the last boundary condition, a new value of λ_1 is chosen and the process is repeated until the correct value of λ_1 is found.

The technique of performing this trial and error method proceeds using the following steps:

(i) Given a wide range of λ_1 (-130 to 130) and A_3 (-200 to 200), for each λ_1, we assign a set of A_3 values and calculate $\psi_1(\pm 1)$ and $\psi_1'(\pm 1)$ by using equation (24a) together with equations (12) and (12a) and plot curves as shown in Fig. 4.2, Fig. 4.3, and Fig. 4.4. From these figures we can predict that the value of A_3 may lie somewhere in the neighborhood of the origin. We then take a smaller range of A_3 values and proceed to the next step.

(ii) Set the range of A_3 from -30 to +30, and assign several values of λ_1. For each value of λ_1, calculate

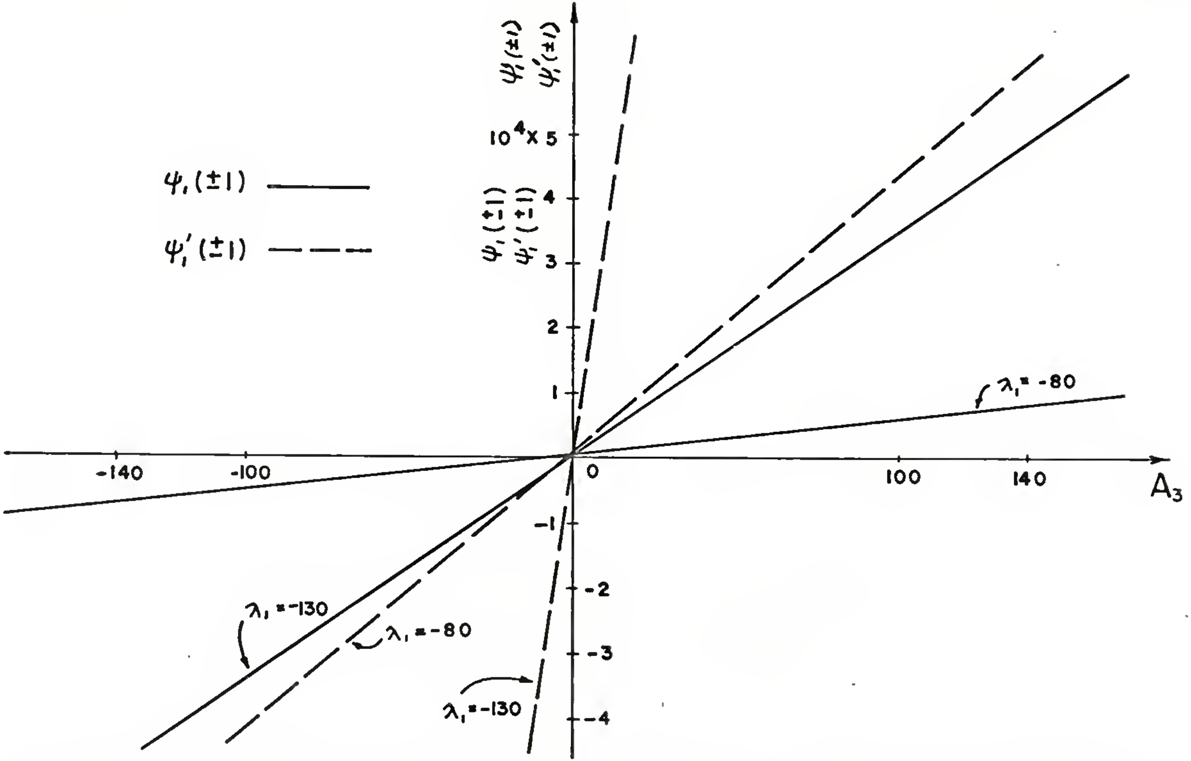

Fig. 4.2. Functions $\psi_1(\pm 1)$ and $\psi_1'(\pm 1)$ with a wide range of A_3 and with a wide range of different values of λ_1 ($\lambda_1 = -130, -80$).

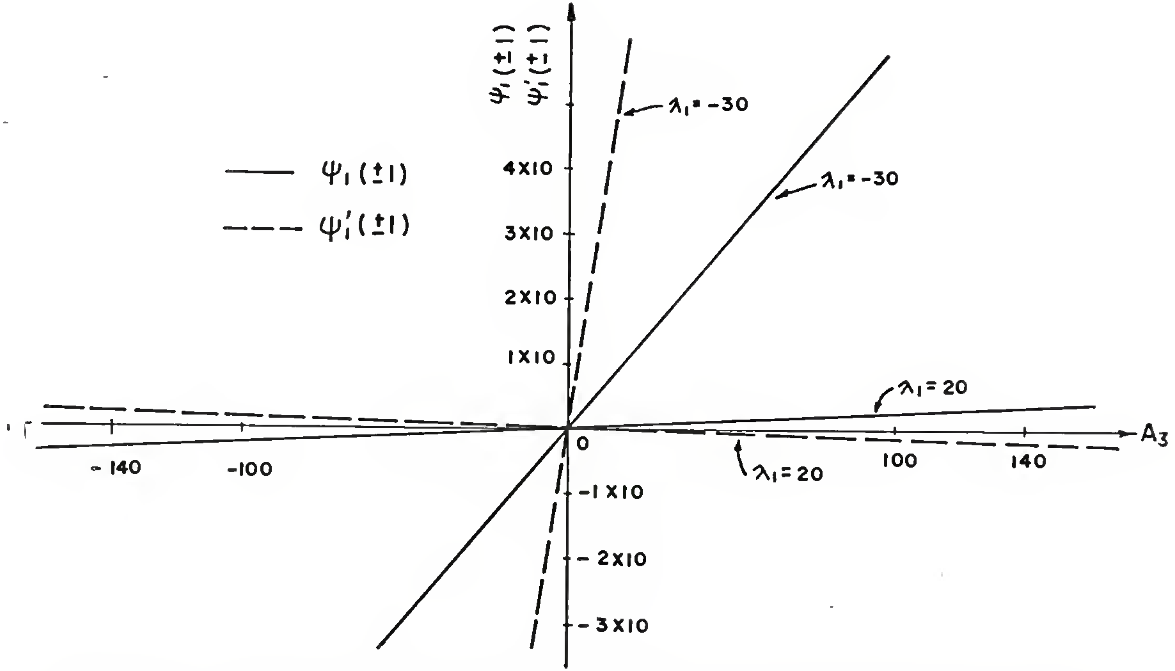

Fig. 4.3. Functions $\psi_1(t_1)$ and $\psi_1'(t_1)$ with a wide range of A_3 and with a wide range of different values of λ_1 ($\lambda_1 = -30, 20$).

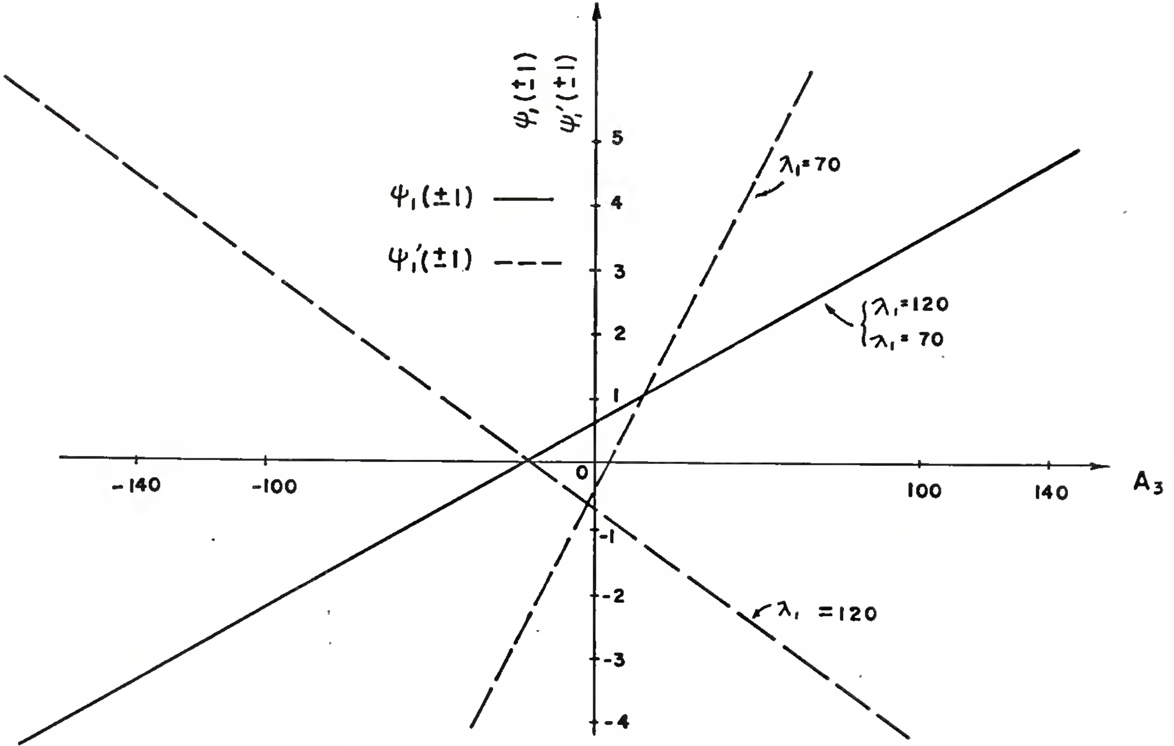

Fig. 4.4. Functions $\psi_1(\pm 1)$ and $\psi_1'(\pm 1)$ with a wide range A_3 and with a wide range of different values of λ_1 ($\lambda_1 = 70, 120$).

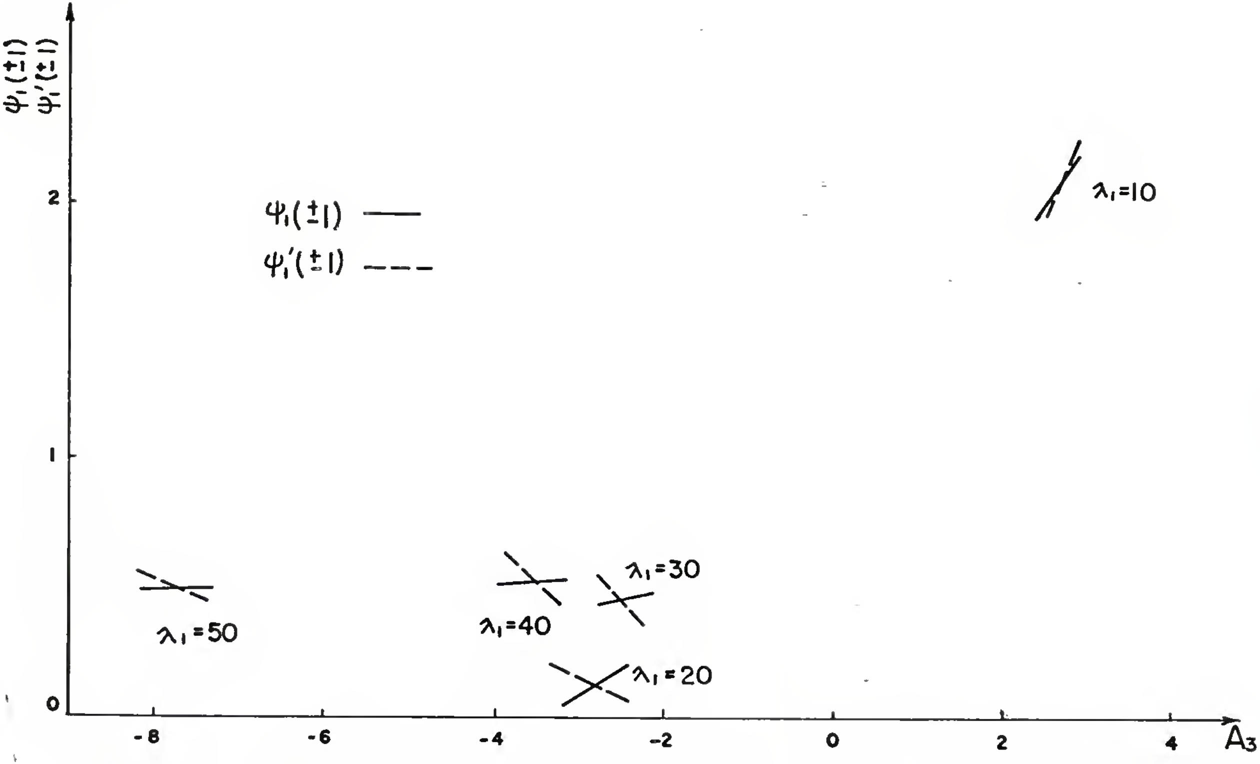

Fig. 4.5. Trace of the intersection point of $\psi_1(\pm 1)$ and $\psi_1'(\pm 1)$ with a wide range of different values of λ_1 and a small range of A_3.

$\psi_1(\pm 1)$ and $\psi_1'(\pm 1)$ as before and trace the intersection points of $\psi_1(\pm 1)$ and $\psi_1'(\pm 1)$ for each λ_1 as shown in Fig. 4.5. From this figure, we can assure that the value of λ_1 is located somewhere between 10 and 20, and that the value of A_3 is located somewhere between -10 and 10.

(iii) From the conclusion of steps (i) and (ii), we can now make a program to find the true value of A_3, which lies between -10 and 10. This is done by assigning a great many values of λ_1 and applying the Chords method [9] (or linear interpolation iterative formula) (see Fig. 4.6) to find the required value of λ_1 and A_3 which can satisfy the boundary condition $\psi_1(\pm 1) = 0$ and $\psi_1'(\pm 1) = 0$. We do not use the Newton iterative formula because the first derivative of $\psi_1(\pm 1)$ which varies with A_3 is difficult to find.

A flow chart to find true value of λ_1 and A_3 is shown in Table 4.6; it is followed by a symbol table (Table 4.7) and a FORTRAN program (Table 4.8), and some output data are shown as in Table 4.9. From these output data we can see that $\lambda_1 = 18.81$, $A_3 = -3.0103658$ are the values which can satisfy the boundary conditions better than any other set of λ_1 and A_3 values.

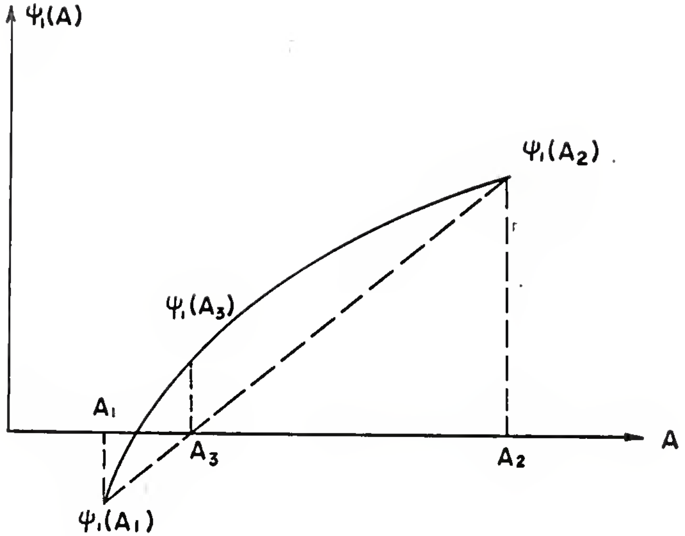

$$A_3 = \frac{\psi_1(A_1)A_2 - \psi_1(A_2)A_1}{\psi_1(A_1) - \psi_1(A_2)}$$

Fig. 4.6. The Chords Method (or linear interpolation iterative formula).

Table 4.6. Flow chart for finding λ_1 and A_3 by trial and error.

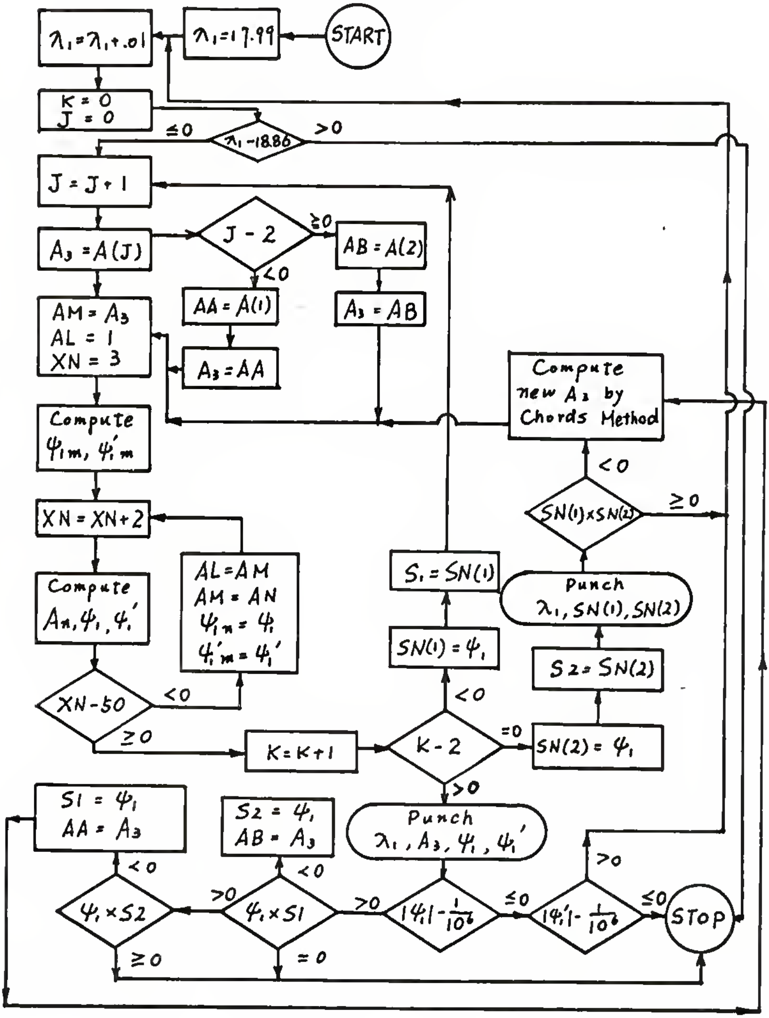

Table 4.7. Symbol Table for finding λ_1 and A_3 by trial and error

Variable	FORTRAN Symbol
λ_1	DM
A_n	AN
A_3	A3
Ψ_1	SFN
Ψ_1'	SF1N
A_{n-2}	AM
A_{n-4}	AL

TABLE 4.8. FORTRAN PROGRAM FOR FINDING λ_1 AND A3 BY TRIAL AND ERROR

```
C   C  MATCHING METHOD--SOLVING DAMDA AND A3 BY TRIAL AND ERROR
  110 FORMAT(E12.5,E16.8,2E14.6)
  118 FORMAT(6E12.5)
  119 FORMAT(/28X,3E14.6)
      DIMENSION A(6),SN(6)
      READ 118,(A(J), J=1,2)
      DM=17.99
    1 DM=DM+.01
      K=0
      J=0
    9 J=J+1
      IF(DM-18.86) 10,10,81
   10 A3=A(J)
      IF(J-2)101,102,102
  101 AA=A(1)
      A3=AA
      GO TO 11
  102 AB=A(2)
      A3=AB
   11 AM=A3
      AL=1.
      XN=3.
      SFM=1.+AM
      SF1M=1.+3.*AM
   12 XN=XN+2.
      AN=3.*DM*((XN-6.)*(XN-3.)*AL-(XN-2.)*(XN-3.)*AM)
      AN=AN/(2.*XN*(XN-1.)*(XN-2.)*(XN-3.))
      SFN=SFM+AN
      SF1N=SFIM+XN*AN
      IF(XN-50.) 20,30,30
   20 AL=AM
      AM=AN
      SFM=SFN
      SF1M=SF1N
      GO TO 12
   30 K=K+1
      IF(K-2)31,32,34
   31 SN(1)=SFN
      S1=SN(1)
      GO TO 9
   32 SN(2)=SFN
      S2=SN(2)
      PUNCH 119, DM,SN(1),SN(2)
      IF(SN(1)*SN(2)-.0)33,1,1
```

```
 33 A3M=(S1*AB-S2*AA)/(S1-S2)
    A3=A3M
    GO TO 11
 34 PUNCH 110, DM,A3,SFN,SF1N
    IF(ABS(SFN)-.0000001)340,340,341
340 IF(ABS(SF1N)-.0000001)81,81,1
341 IF(SFN*S1-.0)35,81,36
 35 S2=SFN
    AB=A3
    GO TO 33
 36 IF(SFN*S2-.0)37,81,81
 37 S1=SFN
    AA=A3
    GO TO 33
 81 STOP
    END
```

INPUT DATA OF A(J)

```
- .10000E+02 0.10000E+02
```

TABLE 4.9. SOME NUMERICAL RESULTS OF λ_1 AND A3 BY TRIAL AND ERROR

```
                                    DM            SN(1)          SN(2)

   DM            A3                 SFN           SF1N

                                .181000E+02 -0.179290E+01  0.322494E+01
.18100E+02 -0.28538818E+01  0.102330E-07 -0.111514

                                .182000E+02 -0.177211E+01  0.320240E+01
.18200E+02 -0.28752463E+01  0.124119E-06 -0.961387E-01
.18200E+02 -0.28752468E+01 -0.184294E-06 -0.961409E-01
.18200E+02 -0.28752465E+01 -0.242940E-07 -0.961402E-01

                                .183000E+02 -0.175145E+01 -0.318002E+01
.18300E+02 -0.28968282E+01 -0.127630E-06 -0.806872E-01
.18300E+02 -0.28968277E+01 -0.616171E-07 -0.806885E-01

                                .184000E+02 -0.173095E+01  0.315780E+01
.18400E+02 -0.29186301E+01 -0.345470E-06 -0.651551E-01
.18400E+02 -0.29186288E+01  0.968014E-08 -0.651544E-01

                                .185000E+02 -0.171060E+01  0.313573E+01
.18500E+02 -0.29406523E+01  0.431958E-07 -0.495396E-01

                                .186000E+02 -0.169036E+01  0.311382E+01
.18600E+02 -0.29629008E+01 -0.857723E-07 -0.338454E-01
                                .187000E+02 -0.167032E+01  0.309207E+01
.18700E+02 -0.29853752E+01  0.738346E-07 -0.180690E-01

                                .187100E+02 -0.166832E+01  0.308991E+01
.18710E+02 -0.29876369E+01 -0.329172E-06 -0.164876E-01
.18710E+02 -0.29876356E+01  0.140046E-06 -0.164872E-01
.18710E+02 -0.29876359E+01  0.173046E-06 -0.164857E-01
.18710E+02 -0.29876362E+01 -0.347957E-07 -0.164858E-01

                                .187200E+02 -0.166632E+01  0.308774E+01
.18720E+02 -0.29898991E+01  0.769620E-08 -0.149028E-01

                                .187300E+02 -0.166433E+01  0.308558E+01
.18730E+02 -0.29921643E+01 -0.275777E-06 -0.133198E-01
.18730E+02 -0.29921632E+01 -0.687473E-07 -0.133206E-01

                                .187400E+02 -0.166233E+01  0.308342E+01
.18740E+02 -0.29944298E+01  0.811064E-07 -0.117360E-01
```

```
                                    DM              SN(1)            SN(2)

    DM                 A3           SFN             SF1N

                                    .187500E+02 -0.166034E+01  0.308125E+01
 .18750E+02 -0.29967006E+01 -0.991142E-07 -0.101486E-01

                                    .187600E+02 -0.165835E+01  0.307910E+01
 .18760E+02 -0.29989716E+01  0.694117E-08 -0.856280E-02

                                    .187700E+02 -0.165636E+01  0.307694E+01
 .18770E+02 -0.30012450E+01  0.248017E-06 -0.697654E-02
 .18770E+02 -0.30012461E+01  0.190590E-07 -0.697484E-02

                                    .187800E+02 -0.165437E+01  0.307478E+01
 .18780E+02 -0.30035229E+01 -0.357000E-06 -0.538865E-02
 .18780E+02 -0.30035215E+01  0.878603E-07 -0.538922E-02

                                    .187900E+02 -0.165238E+01  0.307263E+01
 .18790E+02 -0.30058014E+01 -0.296336E-06 -0.379993E-02
 .18790E+02 -0.30058003E+01  0.131404E-07 -0.379881E-02

                                    .188000E+02 -0.165040E+01  0.307048E+01
 .18800E+02 -0.30080810E+01  0.749293E-07 -0.221165E-02

                                    .188100E+02 -0.164841E+01  0.306833E+01
 .18810E+02 -0.30103658E+01 -0.139789E-06 -0.619150E-03
 .18810E+02 -0.30103653E+01 -0.651258E-07 -0.618435E-03

                                    .188200E+02 -0.164643E+01  0.306618E+01
 .18820E+02 -0.30126518E+01 -0.254073E-06  0.972500E-03
 .18820E+02 -0.30126508E+01  0.176383E-06  0.973849E-03
 .18820E+02 -0.30126512E+01 -0.183617E-06  0.972249E-03
 .18820E+02 -0.30126511E+01 -0.836173E-07  0.972249E-03

                                    .188300E+02 -0.164445E+01  0.306403E+01
 .18830E+02 -0.30149389E+01 -0.755189E-07  0.256444E-02

                                    .188400E+02 -0.164247E+01  0.306188E+01
 .18840E+02 -0.30172282E+01  0.258549E-06  0.415825E-02
 .18840E+02 -0.30172293E+01 -0.775116E-07  0.415768E-02

                                    .188500E+02 -0.164049E+01  0.305974E+01
 .18850E+02 -0.30195229E+01 -0.470679E-06  0.574926E-02
 .18850E+02 -0.30195210E+01  0.276550E-06  0.575088E-02
 .18850E+02 -0.30195217E+01 -0.777869E-07  0.574916E-02

                                    .188600E+02 -0.163852E+01  0.305759E+01
 .18860E+02 -0.30218153E+01  0.488249E-06  0.734686E-02
 .18860E+02 -0.30218175E+01 -0.266742E-06  0.734497E-02
 .18860E+02 -0.30218168E+01  0.865253E-07  0.734666E-02
```

(4) C_1 and ϵ at the Matching Section

As soon as λ_1 and A_3 are found, the values of C_1 and ϵ at the matching section can be obtained by using equations (15) and (16). Eliminating $C_1 e^{-\lambda_1 \epsilon^2}$ from both equations gives a seventh order equation in ϵ as follows [1].

$$\begin{aligned} g(\epsilon) \; = \; & K_1 + \epsilon\left[K_1^2+2K_2-6-\psi_1'''(1)\right] + \epsilon^2\left[3K_1K_2+3K_3+2K_1\psi_1'''(1)\right] \\ & + \epsilon^3\left[4K_1K_3+2K_2^2+4K_4+2K_2\psi_1'''(1)\right] + \epsilon^4\left[5K_1K_4+5K_2K_3\right. \\ & \left.+ 2K_3\psi_1'''(1)\right] + \epsilon^5\left[6K_2K_4+3K_3^3+2K_4\psi_1'''(1)\right] \\ & + 7K_3K_4\epsilon^6 + 4K_4^2\epsilon^7 \; = \; 0 \end{aligned} \qquad (25)$$

The K_1 value has been obtained in the present work as shown in section 4.2-(2). The K_2, K_3, K_4 values are taken from the work of Roidt and Cess [8].

For finding ϵ in equation (25), the Newton-Raphson iteration method [9] is applied (see Fig. 4.7) because $g'(\epsilon)$ can be easily obtained.

After we get ϵ, C_1 is obtained by substituting ϵ into equation (15). A flow chart (Table 4.10) for the entire computation is followed by a symbol table (Table 4.11) and a FORTRAN program (Table 4.12). The computation is also carried out on an IBM 1620 digital computer. The output data are shown in Table 4.13.

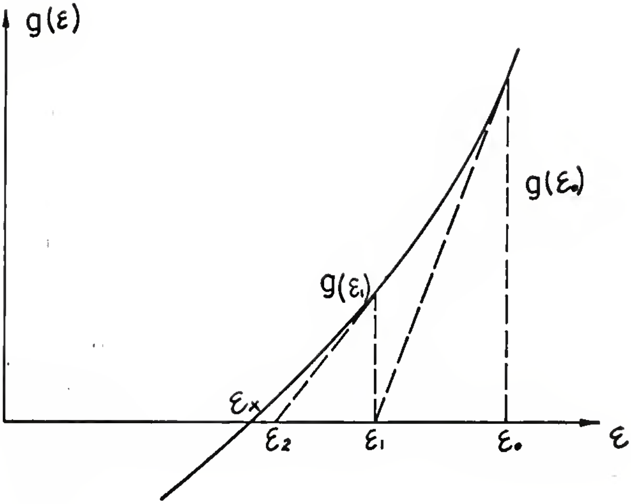

$$\varepsilon_{k+1} = \varepsilon_k - \frac{g(\varepsilon_k)}{g'(\varepsilon_k)}$$

Fig. 4.7. Newton-Raphson's Method.

Table 4.10. Flow chart for solving C_1 and ε.

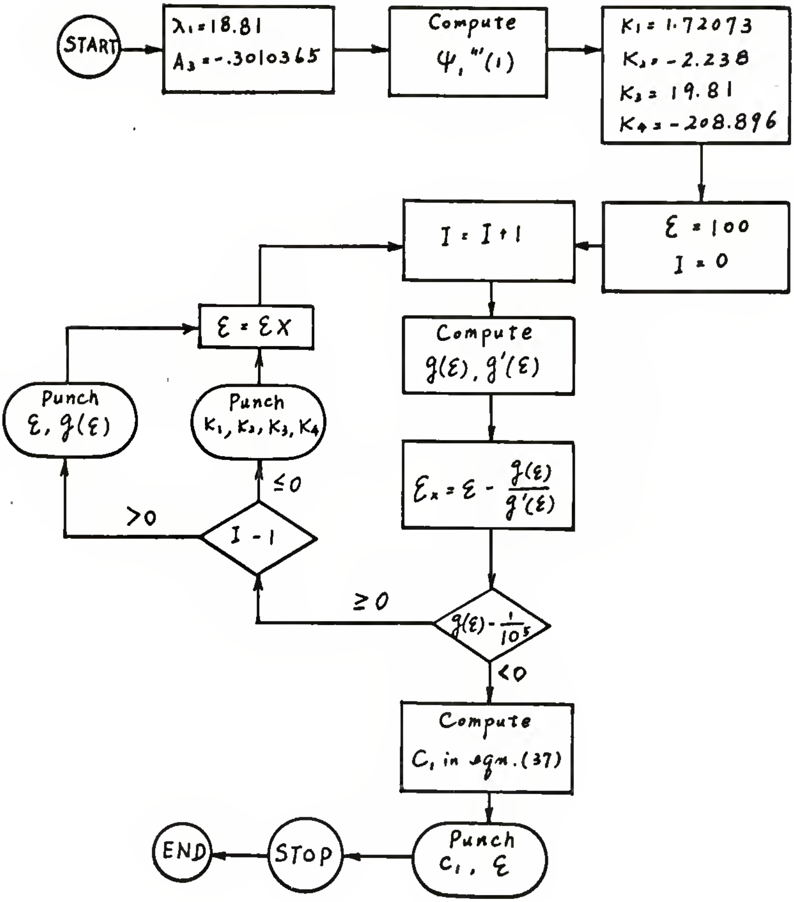

Table 4.11. Symbol Table for Solving C_1 and ϵ

Variable	FORTRAN Symbol
ϵ_{k+1}	EX
ϵ_k	E
$g(\epsilon_k)$ or $g(\epsilon_{k+1})$	G
$g'(\epsilon_k)$ or $g'(\epsilon_{k+1})$	G1
K_1	XK1
K_2	XK2
K_3	XK3
K_4	XK4
λ_1	DM
A_3	A3
$\Psi_1'''(1)$	SF3N
A_n	AN
e	EL
C_1	C1

TABLE 4.12. FORTRAN PROGRAM FOR SOLVING C1 AND ε AT MATCHING SECTION

```
C   C  MATCHING METHOD---SOLVING EPSILON AND C1 AT MATCHING SECTION
  100 FORMAT(4E14.6)
  101 FORMAT(2E14.6)
  102 FORMAT(/3H E=E14.6)
  103 FORMAT(/4H C1=E14.6)
      DM=18.81
      A3=-3.0103653
   11 AM=A3
      AL=1.
      XN=3.
      SF3M=6.*AM
   12 XN=XN+2.
      AN=3.*DM*((XN-6.)*(XN-3.)*AL-(XN-2.)*(XN-3.)*AM)
      AN=AN/(2.*XN*(XN-1.)*(XN-2.)*(XN-3.))
      SF3N=SF3M+XN*(XN-1.)*(XN-2.)*AN
      IF(XN-50.)20,22,22
   20 AL=AM
      AM=AN
      SF3M=SF3N
      GO TO 12
   22 XK1=1.72073
      XK2=-2.238
      XK3=19.81
      XK4=-208.896
   23 B1=XK1*XK1+2.*XK2-6.-SF3N
      B2=3.*XK1*XK2+3.*XK3+2.*XK1*SF3N
      B3=4.*XK1*XK3+2.*XK2*XK2+4.*XK4+2.*XK2*SF3N
      B4=5.*XK1*XK4+5.*XK2*XK3+2.*XK3*SF3N
      B5=6.*XK2*XK4+3.*XK3*XK3+2.*XK4*SF3N
      B6=7.*XK3*XK4
      B7=4.*XK4*XK4
   24 E=100.
      I=0
   30 I=I+1
      G=XK1+E*B1+E*E*B2+E*E*E*B3+E*E*E*E*B4+E*E*E*E*E*B5
      G=G+E*E*E*E*E*E*B6+E*E*E*E*E*E*E*B7
      G1=B1+2.*B2*E+3.*B3*E*E+4.*B4*E*E*E+5.*B5*E*E*E*E
      G1=G1+6.*B6*E*E*E*E*E+7.*B7*E*E*E*E*E*E
      EX=E-G/G1
      IF(ABS(G)-.10000E-04) 50,50,35
   35 IF(I-1) 40,40,41
   40 PUNCH 100, XK1,XK2,XK3,XK4
      GO TO 42
```

```
41 PUNCH 101, E,G
42 E=EX
   GO TO 30
50 EL=2.7182818
   P=DM*E*E
   Q=1.+XK1*E+XK2*E*E+XK3*E*E*E+XK4*E*E*E*E
   C1=(1.5-Q)*EL**P
   PUNCH 102, E
   PUNCH 103, C1
80 STOP
   END
```

TABLE 4.13. SOME OUTPUT DATA FOR C1 AND ε AT MATCHING SECTION

```
   XK1             XK2               XK3              XK4

.172073E+01 -0.223800E+01  0.198100E+02 -0.208896E+03

   E              G

.539884E+02  0.232642E+18
.462792E+02  0.790790E+17
.396713E+02  0.268603E+17
.340374E+02  0.913705E+16
.291526E+02  0.310584E+16
.249913E+02  0.105572E+16
.214245E+02  0.358856E+15
.183673E+02  0.121982E+15
.157468E+02  0.414636E+14
.135007E+02  0.140941E+14
.115755E+02  0.479082E+13
.992527E+01  0.162848E+13
.851082E+01  0.553543E+12
.729845E+01  0.188157E+12
.625929E+01  0.639572E+11
.536860E+01  0.217398E+11
.460517E+01  0.738956E+10
.395083E+01  0.251177E+10
.339000E+01  0.853755E+09
.290933E+01  0.290187E+09
.249738E+01  0.986299E+08
.214435E+01  0.335210E+08
.184184E+01  0.113918E+08
.158267E+01  0.387089E+07
.136068E+01  0.131504E+07
.117063E+01  0.446601E+06
.100803E+01  0.151583E+06
.869081      0.513985E+05
.750592      0.173980E+05
.649912      0.587082E+04
.564920      0.196961E+04
.494040      0.653356E+03
.436323      0.211685E+03
.391598      0.650096E+02
.360582      0.174340E+02
.344082      0.320316E+01
.339413      0.204601
.339072      0.102800E-02

F=   0.339070

C1=   0.188016E+02
```

4.3. Results and Discussion

In 1912 Topfer [6] calculated the $f_0(\eta)$ function by using the Runge-Kutta method; the results were then improved with a high degree of accuracy by Howarth [7] in 1938. In the original paper by Howarth, the method used in the computation was not mentioned. By comparing the present results with those of Howarth we find that there is excellent agreement.

The computation of λ_1 and A_3 by trial and error is extremely difficult; one has to make a great many tests before getting favorable results. Schlichting [10] was the first to find the eigenvalue $\lambda_1 = 18.75$ in 1934; other authors also use the same value, as can be seen from the literature [3, 8]. But from the output data in Table 4.9, we can conclude that $\lambda_1 = 18.81$ is a more accurate one that can satisfy the boundary conditions more accurately.

The values of C_1 and ϵ at the matching section are obtained from the λ_1 value, so that the values of C_1 and ϵ computed in the present work are different from those obtained by other authors as shown in Table 4.14. Some of the results computed in the present work are compared with those obtained by other authors as shown in Table 4.14.

Table 4.14. Comparison of some numerical results in the present work with other authors

Items / Authors	$f''(0)$	K_1	λ_1	A_3	C_1	ϵ^*
Howarth [7]	.33206	-----	-----	-----	-----	-----
Schlichting[10]	-----	1.72	18.75	-----	-0.3485	.1264
Roidt and Cess [8]	-----	1.7209	18.75	-----	-0.452	.1294
Barsness [3]	-----	-----	18.75	-2.996710	-0.4118	.1282
Present Work	.332063	1.72073	18.81	-3.0103653	18.8016	.33907

REFERENCES

1. Li, K. C., "Analytical and Numerical Solutions of Some Entrance Region Flow Problems", M.S. Report, Mech. Engg., Kansas State Univ., Jan. 1966.

2. Schlichting, H., "Boundary Layer Theory", McGraw-Hill, New York, 4th ed., pp. 116-124, pp. 169-171, 1960.

3. Barsness, E. J., "Magnetohydrodynamics Effects Upon Laminar Flow in the Entrance Region of Perfectly Conducting Parallel Plates", M.S. Thesis, University of Pittsburgh, 1960.

4. Nielson, K. L., "Methods in Numerical Analysis", The Macmillan Company, New York, 1964.

5. Blasius, H., "Grenzschichten in Flussigkeiten mit kleiner Reibung", Z. Math. u. Phys. 56, 1 (1908), Engl. Transl. in NACA Tech. Memo No. 1256.

6. Töpfer, C., "Bemerkungen zu dem Aufsatz von H. Blasius, 'Grenzschichten in Flüssigkeiten mit kleiner Reibung'", Z. Math. u. Phys. 60, 397 (1912).

7. Howarth, L., "On the Solution of the Laminar Boundary Layer Equations", Proc. Roy. Soc., London, A164, 547 (1938).

8. Roidt, M. and R. D. Cess, "An Approximate Analysis of Laminar Magnetohydrodynamics in the Entrance Region of a Flat Duct", Trans. of ASME, 84E, J. of Appl. Mech., 29, 171-176 (1962).

9. McCormick, J. M. and M. G. Salvadori, Numerical Methods in FORTRAN, Prentice-Hall, Inc., Englewood Cliffs, New Jersey, 1964.

10. Schlichting, H., "Laminare Kanuleinlaufströmung", ZAMA, 14, 368-373 (1934).

ACKNOWLEDGEMENT

The author wishes to express his sincere gratitude to his major advisor, Dr. C. L. Hwang, for his constant encouragement, advice, and valuable suggestions; Dr. L. T. Fan, Professor of Chemical Engineering, for his enthusiastic support and valuable suggestions; Dr. R. G. Nevins, Head of the Department of Mechanical Engineering, Dr. Wilson Tripp, Professor of Mechanical Engineering, and Dr. S. T. Parker, Professor of Mathematics, for being members of the author's advisory committee; the Air Force Office of Scientific Research Grant AF-AFOSR-463-66 for partly supporting this work.

The author sincerely appreciates the assistance given by Dr. L. E. Erickson, Assistant Professor of Chemical Engineering, and by Mr. Grant Fox in Chemical Engineering. Appreciation goes to Professor Smaltz for giving computing time on the IBM 1620 computer.

COMPUTATIONAL ASPECTS OF SOME ENTRANCE REGION FLOW PROBLEMS

by

CHING-TAI LU

B.S., Taiwan Provincial Cheng-Kung University, 1958

AN ABSTRACT OF A MASTER'S REPORT

submitted in partial fulfillment of the

requirements for the degree

MASTER OF SCIENCE

Department of Mechanical Engineering

KANSAS STATE UNIVERSITY
Manhattan, Kansas

1967

The study of the developing velocity profiles and pressure drops in the hydrodynamic entrance region of tubes and ducts has attracted the interests of investigators for many years. Although the exact analytical solution is not available, many approximate solutions have been presented. The approximation methods of solution can be classified into four different categories: the momentum integral method, the linearizing method, the matching method, and the finite difference method.

The purpose of this report is to present a detailed computational study of the momentum integral method, the linearizing method, and the matching method by using a high speed digital computer. The computational procedures, flow charts, FORTRAN programs and results in each method are presented in detail and some of the results are compared with those obtained by other authors.

The main numerical methods used in this work are numerical integration, series solution of differential equations, eigenvalue solutions and the evaluation of modified Bessel functions. In Chapter 2 Schiller's solution by the momentum integral method for a flow in a circular tube is described. It is then followed by computational procedures to compute the velocity profiles, pressure drops and entrance length in the whole entrance region. All computations are done using only one FORTRAN program and are carried out on an IBM 1620 digital computer.

Chapter 3 contains a description of Langhaar's linearization method for the flow in a circular tube. The nonlinear partial differential equation of motion for the axial direction is linearized by the assumption that the convective terms are a function of axial direction only. The solution is presented in closed form in terms of modified Bessel functions. The evaluation of modified Bessel functions and the trapezoidal rule for numerical integration are used in this chapter to obtain the numerical results. In order to make the computation clear, three separate FORTRAN programs are used to compute entrance length, velocity profiles and pressure drops. The results are compared with those obtained by Langhaar.

Chapter 4 deals with Schlichting's matching method. In this method the flow field is divided into two sections; the upstream and downstream sections. In the upstream section, a boundary layer formulation of equations is used and a solution developed in a series stream function with Blasius' functions as coefficients. When this solution becomes unwieldy, an exponential velocity deviation from the fully developed flow is assumed and joined to the boundary layer solution to complete the description of the flow. The Runge-Kutta integration method, the Newton-Raphson iteration method, and the Chords method (or linear interpolation iterative formula) are applied in this chapter to obtain the numerical results for the entire entrance region. The results are then compared with those obtained by other authors.